Design and Evaluation of Dynamic Field-of-View Restriction Techniques to Mitigate Cybersickness in Virtual Reality

A DISSERTATION
SUBMITTED TO THE FACULTY OF THE GRADUATE SCHOOL
OF THE UNIVERSITY OF MINNESOTA
BY

Fei Wu

IN PARTIAL FULFILLMENT OF THE REQUIREMENTS
FOR THE DEGREE OF
Doctor of Philosophy

Under the supervision of Evan Suma Rosenberg

September, 2022

Acknowledgements

Many people have earned my gratitude for their contributions to my graduate school experience.

I'd like to thank Evan Suma Rosenberg, my advisor, for his inspiration, guidance, and support. When I was discouraged with research work and lost confidence in pursuing a Ph.D., he was the person who first made me realize that I was capable of doing research and finishing my degree. He was always there to encourage me when I ran into problems with my research and was always complimentary about the outcomes of my work.

The other members of my thesis committee, Victoria Interrante, Daniel Keefe, and Tom Stoffregen, have also been extremely helpful. They have provided unique insight and assistance that has had a significant impact on my dissertation and my time as a Ph.D. student.

I'd also like to thank everyone at the University of Minnesota's Illusioneering Lab. Their kindness and encouragement have made my time at the University of Minnesota a lot more enjoyable.

I'm grateful to my friends and professors at Zhejiang University. They open my eyes to the fact that, as a woman, I should be free of the prejudices I was raised with and have an equal opportunity to earn a doctorate.

Finally, I'd like to express my gratitude to my family for their love and support.

Dedication

To my family and friends who have loved and supported me over the years

Abstract

Although virtual reality has been gaining in popularity, users continue to report discomfort during and after the use of VR applications, and many experience symptoms associated with cybersickness. To mitigate this problem, dynamic field-of-view (FOV) restriction is a common technique that has been widely implemented in commercial VR games. FOV restriction artificially reduces the field of view during movement to limit optical flows and reduce discomfort caused by the mismatch between virtual motion and physical motion. FOV restriction has been shown in numerous studies to improve comfort and enhance user experience in virtual reality.

The standard dynamic FOV restriction is created by adding a symmetrical black opaque mask at the periphery of the user's filed-of-view and its size changes only with the user's virtual velocity. It does not take into account any differences in users, virtual environments, or other usage conditions. This simplistic implementation leads to some limitations. The first limitation is that the FOV restriction reduces users' visibility of the virtual environment and can negatively impact their subjective experience. The second limitation is that the unblocked imagery when applying restrictor is usually in the center of the field of view, which is incompatible with the users' eye movements during locomotion. The third limitation is that the classical restrictor is scaled by the velocity and angular velocity of users' virtual movements. This design assumes that users feel the same cybersickness when they experience the same velocity, which is unrealistic. Beyond these limitations, there is a lack of scientific understanding of how to effectively apply FOV restrictions for different types of virtual environments and virtual motions.

This thesis presents four major contributions to the existing dynamic FOV restriction research. First, I present a novel technique known as passthrough

FOV restriction, which combines the dynamic field of view modification with rest frames generated from 3D scans of the physical environment. The informal testing suggests that this approach is a promising method for reducing motion sickness and improving user safety at the same time. Secondly, I present a novel asymmetric field-of-view restrictor known as the ground-visible restrictor, which maintains the visibility of the ground plane during movement. User studies showed that ground-visible FOV restriction offers benefits for user comfort, postural stability, and a subjective sense of presence. Thirdly, I provide another variant of FOV restriction, referred to as the side restrictor, which expands side visibility and maintains restriction during rotation. A user study evaluated the new technology and demonstrated its benefits in reducing cybersickness and discomfort and improving visibility. Finally, I present an adaptive restrictor that uses the optical flow amount to determine the position and size of the restriction. A mixed design study investigated its performance and confirmed its superiority over traditional restrictors in providing a better subjective user experience.

Contents

List of Tables

List of Figures

Chapter 1

Introduction

1.1 Cybersickness in Virtual Reality

In recent years, virtual reality (VR) technology has developed rapidly. It has been widely used in entertainment, healthcare, education, and commercial activities. However, many users report discomfort during and after using VR applications and experience symptoms associated with motion sickness, such as nausea, vertigo, sweating, headache, eyestrain, etc. Those symptoms may manifest as aftereffects in the hours following the VR experience. Symptoms can last for hours or even days in many cases. Users who encounter so-called "cybersickness" may discontinue the experience early or potentially avoid trying a VR system again in the future.

The mismatch between physical and virtual movements is commonly acknowledged as a major factor that contributes to visually-induced motion sickness in virtual reality. In a VR application, users' virtual motions may not perfectly match their physical movements in the real world. These discrepancies may be unintentional due to technological factors such as tracking error or system latency, or they may be the result of design decisions made by content creators. For example, virtual locomotion techniques are commonly implemented using handheld controllers to allow movement through virtual environments that are larger than

the real-world workspace. Because virtual locomotion is such an essential technique for users with limited physical space, cybersickness becomes an unavoidable issue. Users also suffer from other forms of discomfort besides cybersickness due to the nature of virtual locomotion.

In addition, the physical discomfort can reduce task performance and the effectiveness of virtual reality applications [1]. Scientific evidence was found that cybersickness has a negative relationship with presence; users who suffer from cybersickness have a lower sense of presence in virtual environments [2]. Furthermore, many studies have documented biological sex differences in motion sickness [3], with motion sickness more prevalent among women than among men. This phenomenon introduces important accessibility concerns, especially as immersive technologies become more widely used in work-related contexts.

1.2 Field-of-View Restriction

Field-of-view restriction has been proved to be a useful tool to mitigate cybersickness and integrated into many commercial VR applications. It decreases the amount of the optical flow by reducing the size of the field-of-view, thus eliminating the cybersickness caused by the mismatch between the visual and vestibular systems.

Field of View (FOV) is the extent of the observable world seen at any given moment. In head-mounted displays (hmds), the FOV is altered based on the physiological parameters detected by a sensor comprised by the computer system. Many research has noted a positive correlation between FOV size and cybersickness. When the size of FOV increases, the optical flow increases as well. A large and frequently changing optic flow that simulates the direction and speed of self-motion should produce significant and sustained mismatch between physical and virtual motions in a stationary observer. Accordingly, a larger FOV leads to a more severe cybersickness. Previous researchers also have noted a positive correlation between FOV size and sense of presence. An adequate FOV increases the

user's visibility and enhances the user's sense of immersion, resulting in a better user experience.

Dynamic field-of-view restriction, also known as "tunneling," is one of the most popular techniques to mitigate cybersickness and has been widely used in commercial VR games [4, 5]. This approach partially obscures the user's visual field by displaying a black opaque texture mask in the periphery that dynamically changes size according to movement velocity, as shown in Figure 1.1.

Optical flow is a perceptual cue widely thought to be associated with visually-induced motion sickness. It is the pattern of the image sequence of moving objects between two consecutive frames caused by object or users' movement in a virtual environment. The optical flow allows users to have a sensation of illusory self-motion. When lacking physical movements, this sensation of illusory self-motion, known as *vection*, plays as a main contributor to the cybersickness [6]. The FOV restrictor obscures a portion of the user's vision to reduce the amount of optical flow received by the user's visual system, lowering the user's level of cybersickness.

In a formal study, Fernandes and Feiner confirmed that a dynamic FOV restrictor indeed reduces discomfort during virtual locomotion [5]. Teixeira and Palmisano [7] also claimed that dynamic FOV restriction can serve as a viable countermeasure to cybersickness.

Dynamic FOV restriction has many advantages in reducing cybersickness and has been added to many commercial VR applications. It does not require additional equipment and can be integrated directly into existing commercial VR devices, making it very user-friendly for the general public. The technology also does not have requirements for the user's physical environment and can be used in any situation. The restrictor design does not require much computation, and the color of the restrictor is similar to the one at the edge of the VR device, so it does not slow down the frame rate and does not impact the VR content too much. The restrictor has been proven by many studies to have a good effect on reducing discomfort [5, 8]. According to some studies, the dynamic FOV restrictor can effectively reduce cybersickness in VR [7] and are valid for both sexes [9].

Figure 1.1: Dynamic Field-Of-View restrictor

Some studies have also found that the dynamic FOV restrictor benefits in reducing cybersickness within 360° videos [10, 11].

Although restricting the field-of-view while moving is a typical method of reducing cybersickness, the traditional FOV restrictor was designed in a fairly naive manner. In academia, FOV restriction research is scarce, as well as systematic and thorough studies. In addition, not all studies have formed consistent results. In the meantime, despite the FOV restriction approach has been widely used in commercial games, industries lack scientific expertise to evaluate the performance of these strategies.

1.3 Contributions

In this dissertation, I identify and provide solutions to address limitations in current FOV restriction design, as well as different ways to mitigate cybersickness in virtual reality by designing the FOV restrictor, exploring restrictors that are more adaptive to the user's eye movements, conducive to maintaining postural stability, and provide better visibility. To the best of my knowledge, this is the first comprehensive research of asymmetric field-of-view restrictors and the scientific evidence for their performance in comparison to the traditional symmetric restrictor. The primary outcomes are:

- A unique asymmetric FOV restrictor that combines obstacle avoidance with FOV restriction.
- Two innovative variants of FOV restrictions using asymmetric masks to obscure portions of the periphery while leaving the remaining region unobscured.
- A novel adaptive FOV restrictor that adjusts its position, size, and shape in response to the amount of optical flow.
- Three formal scientific experiments evaluating the FOV restrictor's performance in terms of cybersickness, presence, visibility, postural stability, and task performance.

1.3.1 Passthrough FOV Restriction

The traditional symmetrical restrictor is designed with a black opaque mask that obscures the user's peripheral vision, wasting a portion of the field of view. Simultaneously, when users are immersed in the virtual world, they are unable to see objects in the physical world and are thus frequently prone to colliding with obstacles physically. To utilize peripheral vision and help users avoid obstacles

in the physical world, chapter 3 presents work proposed to combine FOV restriction with obstacle avoidance. In this work, I use the 3D model of the physical environment as the peripheral of FOV instead of a solid black background. This technology maintains the performance of the restriction while adding obstacle avoidance. Besides, this restrictor is an earth referent, that is, it is an element that is stationary with respect to the earth, not with respect to the camera or hmds as is the case with traditional restrictors. The earth referent facilitates the user to maintain postural stability, which has a better effect on reducing cybersickness. The work presented in this chapter was originally published at the 2019 IEEE VR Conference on Virtual Reality and 3D User Interfaces WISP Workshop with the title, "Combining Dynamic Field of View Modification with Physical Obstacle Avoidance" [12].

1.3.2 Asymmetric Restriction

The traditional FOV restrictor is designed as a symmetric mask located in the center of the user's field-of-view. It blocks the ground that provides the necessary postural stability for the user while walking. In addition, users need a side view of the direction of the turn to determine the situation in the direction of the upcoming turn, such as the turn position, obstacles, etc. The symmetrical FOV restrictor obscures the user's side view, therefore causing difficulties for users' virtual turning. In chapter 4 and chapter 5, I propose two asymmetric FOV restrictors that block only a portion of the periphery in the user's FOV, providing better visibility in the virtual motion.

Chapter 4 proposes and evaluates a novel variant of FOV restriction, which I refer to as the *ground-visible restrictor*. This technique uses an asymmetric mask that obscures the upper and side regions of the periphery but leaves the lower region unoccluded. A study was conducted to compare the ground-visible restrictor with the standard symmetric FOV restrictor during navigation through a complex maze-like virtual environment. The results showed that the ground-visible

restrictor can improve user comfort during virtual locomotion, and also provides benefits for postural stability and subjective sense of presence. Furthermore, there were no negative effects observed compared to the traditional symmetric restrictor, and I conclude that the ground-visible technique appears to be a generally superior form of FOV restriction. The work presented in this chapter was originally published at the 2021 ACM Symposium on Spatial User Interaction with the title, "Don't Block the Ground: Reducing Discomfort in Virtual Reality with an Asymmetric Field-of-View Restrictor" where it won the Best Paper Honorable Mention Award [13].

Chapter 5 proposed and evaluated a novel variant of FOV restriction, referred to as a *side restrictor*. Side restriction uses an asymmetric mask to obscure only one side region of the periphery during virtual rotation and laterally shifts the center of restriction towards the direction of the turn. I conducted a study using a between-subjects design that compared the side restrictor, a traditional symmetric restrictor, and a control condition without FOV restriction. Participants were required to navigate through a complex maze-like environment using a controller using one of three restrictors. Compared to the control condition, the side restrictor was effective in mitigating cybersickness, reducing discomfort, improving subjective visibility, and enabling users to remain immersed for a longer period. The work presented in this chapter was originally published at the 2022 IEEE VR Conference on Virtual Reality and 3D User Interfaces with the title, "Asymmetric Lateral Field-of-View Restriction to Mitigate Cybersickness During Virtual Turns" [14].

1.3.3 Adaptive Restriction

The current FOV restrictor design is triggered and scaled based on users' virtual velocity. However, because different environments generate different amounts of optical flow at the same speed, the design of this restrictor may not be appropriate for all virtual environments. Excessive resizing of the field of view in a more open

environment is also likely to cause cybersickness due to changes in the texture of the restrictor. To reduce these effects, the FOV restrictor should be adaptive to different virtual environments and be able to scale according to the optical flow generated in real-time.

Chapter 6 proposes and evaluates a novel variant of FOV restriction, referred to as an *adaptive restrictor*. Adaptive restriction triggers an asymmetric mask to the obscure region of the periphery with the highest optical flow during virtual locomotion. I conducted a study using a mixed design that compared the adaptive restrictor, a traditional symmetric restrictor, and a control condition without FOV restriction and evaluated their performance in a close-quarter virtual environment and an open virtual environment. Participants were instructed to virtually navigate a complex maze-like environment using a controller to experience three sessions, using all three restrictions in sequence and experiencing one of the two environments. The experimental results showed that the adaptive restrictor has a similar effect in reducing discomfort compared to the symmetric restrictor, while also obscuring less of the field-of-view, therefore providing a greater advantage in improving subjective visibility and sense of presence, and allowing users to maintain longer immersions. It suggests that adaptive restriction is an effective cybersickness mitigation technique for virtual locomotion. The work presented in this chapter is under review for publication at the time of writing.

Chapter 2

Related work

2.1 Cybersickness Causes and Symptoms

Motion sickness is a natural response of otherwise healthy individuals that can happen in unfamiliar motion environments. Historically, motion sickness has been associated with inertial motions that characterize vehicular travel (e.g., seasickness). Increasingly, motion sickness is a problem with motions that are visual rather than inertial, which are commonplace in video games, virtual environments, VR systems, remotely operated vehicles, and numerous other interactive technologies. In the context of virtual reality, cybersickness has been publicly acknowledged (e.g., by Oculus and other headset manufacturers) as a major limiting factor of contemporary interactive technologies [15].

Cybersickness has similar symptoms and causes motion sickness. The symptoms include nausea, oculomotor, and/or disorientation induced by any visual stimuli. The commonly postulated causes of cybersickness are a sensory mismatch and postural instability [16].

2.1.1 Sensory Conflict Theory

The sensory conflict theory claims that motion sickness is caused by a mismatch between current patterns of sensory input about self-motion and expected patterns based on previous experience. In the context of virtual reality, visually induced motion sickness is often associated with virtual imagery that does not correlate with the physical motion of the body [1,17]. The sensation of illusory self-motion in the absence of physical movement, also known as vection, has been discussed in many studies related to visually induced motion sickness [6,18]. Since physical movement is typically absent or limited during the VR experience, it should be no surprise that virtual motion is capable of inducing motion sickness.

2.1.2 Postural Instability Theory

According to the postural instability theory, the loss of postural control is not only a consequence but also a causative factor for motion sickness [19]. A subsidiary hypothesis is that the degree of motion sickness is proportional to the amount of postural instability, which can be manipulated by physical restraint. Differences in postural sway have been observed during exposure to potentially nauseogenic motion in a variety of contexts, such as during stance in a moving room [20], during use of console video games [21], and while wearing a virtual reality headset [22].

2.1.3 Other Theories

Many other theories have been proposed to explain the causes of cybersickess from a variety of perspectives.

The vergence-accommodation conflict has long been posited to lead to visual discomfort. Images are displayed at a constant optical distance on one plane in HMDs, while the distance of the virtual objects varies [23].

Eye movements can also induce optic nerve tremors (OKN). Moving visual patterns can innervate the vagus nerve, which has also been described as a potential source of motion sickness [24].

The differences in virtual and physical head pose (DVP) are another cause of the cybersickness in virtual reality devices [25]. This recent study showed that the large magnitude, time-varying patterns of DVP can trigger severe cybersickness. This continuous pattern can also be used to predict the user's cybersickness severity.

2.1.4 Role of Optical Flow

Regardless of its etiological causes, there exists substantial evidence that optical flow is a major contributing factor for visually induced motion sickness. Optical flow is generated by the stimulus of moving visual contents and allows users to experience illusory self-motion, which induces vection when users immerse in the virtual environment without physical movement. Vection plays the main contributor to motion sickness. Studies have found that users who experienced stronger vection also reported more severe cybersickness and therefore vection might be used to identify those who are more susceptible to cybersickness [26, 27]. Therefore, optical flow of self-motion increases the probability of sickness in virtual environments; high rates of optical flow results in significantly higher rates of sickness [17] and this positive relationship is present in both central and peripheral vision [28]. This may be due to the fact that optic flow stimuli can be sensitive to down-weight vestibular signals [29]. The relationship between optical flow and motion sickness has been extensively studied in different aspects, and many parameters are proposed to have an impact on the intensity of motion sickness induced by optical flow, such as the speed of virtual motion [30], the axis of motion [31] and the direction of optical flow [32].

2.2 Cybersickness Measurement

The measurement of cybersickness is challenging. A variety of symptoms are internal, non-observable, and subjective. Additionally, the constellation of symptoms develops over periods, ranging from a few minutes to several hours [33]. Many methods can detect and rate the level of cybersickness, including subjective measurements and objective measurements. The most common subjective measurements are questionnaires that measure users feeling by Likert scales or free questions. The objective measurements include postural stability and physiological state.

2.2.1 Questionnaires

The simulator sickness questionnaire (SSQ) is the most popular questionnaire to measure cybersickness. It was developed by Kennedy et al. in 1993 [34], consisting of 15 simulator sickness symptoms and asking for the severity of symptoms on a 7-point Liker scale. The scores are computed for three categories with weights. Users will be required to fill in a pre-test SSQ before the studies and a post-test SSQ after the study. The delta scores are calculated using the pre-test and post-test results. However, the SSQ is designed to measure the level of simulator sickness, while some research indicated that the symptoms of cybersickness in VR are not the same as simulator sickness [16].

Fast Motion Sickness (FMS) is the other famous questionnaire. It is usually used to monitor participants during the virtual reality experience [35]. The FMS consists of a report of discomfort level on a 1-20 scale. It can be provided in writing or verbally.

Other questionnaires analyzing the cybersickness symptoms are used in some studies, such as the misery scale (MISC) [36].

2.2.2 Postural Stability and Postural Sway

Although less common, some objective measures have also been applied in VR studies. Postural stability became an objective measure since it is a possible cause of cybersickness. Postural stability detection requires participants to stand on a force plate before they are exposed to the virtual environment. The records are the center of foot pressure (CoP) along the anterior-posterior (AP) and medi-olateral (ML) axes continuously for 60 seconds. The measurement process breaks if participants failed to maintain their stance.

Postural sway became an alternative measurement due to the drawbacks of postural stability measurement. Postural sway is usually measured by detecting the body rotation on the x and z-axis. The standard deviation of head movement along an axis is related to the degree of motion sickness, in particular, the standard deviation in the fore-aft axis (Z-axis) increases with the degree of motion sickness [37]. Some research also shows that the velocity of head movement along with an axis increases when the user feels discomfort [38]. Risi et al. found that users feeling sick displayed different postural activity than those who remained well [39]. The results suggested that individuals who are more susceptible to HMD-based cybersickness can be identified based on their spontaneous postural sway.

2.2.3 Physiological Signals

A variety of physiological signals have been used to detect cybersickness symptoms severity [40]. The most commonly used signals include electrocardiogram (ECG), electrogastrogram (EGG), blood pressure, heart rate, respiration (RSP), electroencephalograms (EEG), and skin temperature. These signals are detected by sensors attached to the skin.

2.3 Mitigating Cybersickness in Virtual Reality

A variety of methods have been previously proposed to avoid or mitigate symptoms of cybersickness. Most methods concentrate on visual content and locomotion techniques.

2.3.1 Visual Content

The first category focuses on addressing technological shortcomings that are associated with visual content.

Some techniques are designed to reduce the cybersickness based on the mismatch between physical and virtual motion by altering the optical flow pattern, such as applying a Gaussian blur to the entire presented view during rapid movements [41], to apply a static blur in only the peripheral region [42], to selectively blur pre-defined parts of a scene [43], or to dynamically detect and pre-emptively mask regions of high optical flow in user's visual field [44]. Helmut Buhler et. al evaluated two peripheral visual effects to reduce optical flow in peripheral with head-mounted displays [45]. Farmani et al. evaluated two discrete motion techniques aimed at reducing optical flow through inconsistent displacements [46]. Park et al. mixed the reverse optical flow visually with the virtual visual motion to reduce cybersickness [47]. Bala et al. utilized the amount of optical flow to determine the radius of field-of-view in 360° video [48]. Dynamic FOV restriction is the most popular technique in commercial VR games to reduce optical flow in peripheral regions [5], as discussed in detail in section 2.4.

Scene content also affects the degree of cybersickness to a certain extent. Some research found a decrease in cybersickness if participants move over the flattening environment, such as a planar [49]. Scene content around the center produced less discomfort than off-center focus contents, consistent with the theory that eye movements induce cybersickness [50].

Latency has long been a concern for VR developers, and dynamic variations have been particularly implicated in cybersickness [51], especially at frequencies

near 0.2Hz [52] [53]. Also, some research has found reduced levels of cybersickness when visuals are presented in 2D rather than in stereo [54] which is consistent with the vergency-accommodation conflict theory.

2.3.2 Locomotion

Cybersickness is most commonly associated with virtual locomotion techniques, although some can occur when the user's viewpoint maintains a 1:1 mapping with physical body motion. The locomotion velocity is associated with the cybersickness level because the increase in speed triggers an increase in optical flow. A common approach is to avoid continuous visual representations of motion by requiring the user to teleport in the virtual environment [55] [56], although this is often tedious and can lead to diminished spatial awareness [57]. Several variants on this theme have been explored, including "viewpoint snapping" [58], "jumping" [59], "dashing" [60], and "blinking" [61].

Natural walking [62] or physically body/head movement [63] produces less discomfort than using the controller. Various devices have been used in different studies to assist users with natural walking or head movements, such as a treadmill [64], proprioceptive vibrations [65], and a floor vibration [66]. Navigation modes and controls may also alter the degree of cybersickness. Some researchers have noted a reduced incidence of cybersickness when smoothed virtual motions are presented during the virtual traversal of terrain that would normally afford a bumpier trajectory [67].

2.3.3 Other Techniques

Numerous techniques have been proposed to explore the possibility of reducing cybersickness in many aspects. Some of them are less studied or have no uniform results.

The explicit use of passive restraints is a related but somewhat less practical cybersickness mitigation strategy that has been studied in the context of postural

stability [68].

Motion control is an important factor in addressing the level of cybersickness [69]. Users in control of the virtual movement are less likely to experience cybersickness compared to users who cannot control the viewpoint and orientation, as known as the "driver-passenger effect" [70] [37]. However, a recent study showed the opposite results in VR driving simulations, concluding that the controlling metaphor and whether its feedback matches the user's expectations affects the outcome of motion control [71].

Some studies found that the unrealistic scenes had lower cybersickness than the realism because the user's visual and vestibular cues are unlikely to have prior experience [72] [73].

The possibility of using a deep learning framework to detect and reduce the level of cybersickness in real time has been proposed in some studies [74] [75]. However, no mature framework has been published yet.

2.4 Filed-of-View Restriction

2.4.1 Rest Frame

Related to the idea of focusing attention away from the periphery, it has long been recognized that stable elements, referred to as "rest frames" may help reduce cybersickness [76] [77]. Many studies have indicated that introducing an independent visual background may reduce cybersickness. Varying implementations have been proposed. Duh, et al. proposed several independent grids that fill the entire field of view [78]. A natural independent visual background (IVB) which comprised of clouds was shown to alleviate nausea more effectively than a fixed grid background [79]. An experiment was conducted that confirmed the hypothesis. A small reticle superimposed over the center of the visual field was implemented in [80]. Similarly, Wienrich et al. [81] proposed a fixed virtual nose which increased the experience period and decreased the sickness scores. The

virtual note is in the head reference frame rather than in the real-world reference frame, which is different from a typical rest frame. Chang et al. [82] found that using grid lines decreases cybersickness with EEG detection. I also proposed a wireframe model of the physical world in the periphery [12], which isdescribe in detail in Chapter 3.

The performance of static and dynamic rest frames was studied by [83]. They concluded that a virtual environment with a static or dynamic rest frame allowed users to travel through more waypoints before stopping due to discomfort compared to a virtual environment without a rest frame. Further, a virtual environment with a static rest frame was also found to result in more real-time reported comfort than when there was no rest frame. However, they were not able to verify that the addition of a dynamic rest frame is as effective as a static one.

While much of this research has been done using rotating drums or projection-based displays, similar effects have also been verified in the context of VR headsets [83]. While the mechanism by which rest frames achieve their sickness-mitigating effects is not yet fully understood [84], both eye movements and postural stability appear to also be affected, as stationary eye fixation also helps to stabilize posture [85].

2.4.2 Symmetric FOV restriction

Dynamic FOV restriction has become one of the most widely used mitigation strategies during virtual locomotion [4, 5]. This technique is based on the hypothesis that peripheral optical flow is an aggravating factor for cybersickness. This technique dynamically reduced the displayed FOV in a head-mounted display. The size of the field of view was adjusted based on the velocity of virtual movement. An experiment was conducted to show that this technique can provide advantages to reducing motion sickness during artificial locomotion and improved

sense of presence compared with the static frame. FOV restriction is equally effective in mitigating VR sickness for both sexes [9], and no sex differences in VR sickness incidence were found [86].

A similar technique came up with by [87], in which a dynamical blurring was applied to the periphery area of the retina instead of a black background. They contributed with a saliency detection method based on deep learning to dynamically blur the display in real-time. They experimented to illustrate that this technique can effectively prevent visually induced motion sickness in VR, especially working the high-speed case.

Some studies address how FOV size is determined. The cybersickness relief virtual environment was proposed in [88]. The system managed the field of view based on an artificial neural network whose inputs were the electrophysiological signals of the subject in a virtual environment. An experiment suggested that the system can be a countermeasure against motion sickness.

However, FOV restriction is not without potential downsides, and current approaches have not proven beneficial under all circumstances [89] [90]. In particular, FOV restriction may not be desirable in the nasal portion of the periphery in the view from each eye, and vertical FOV restriction might be inadvisable to the extent that it occludes the ground plane and horizon line, which people may rely on as a stable reference [91]. Some researchers have instead suggested employing strategies that focus attentional resources on the foveal region without explicitly occluding the periphery [92]. In chapter 4, the proposed ground-visible restrictor is intended to address these concerns.

2.4.3 Asymmetric FOV restriction

Recently, some studies have also started to focus on asymmetric FOV restriction. Horizontal FOV plays an important role in providing spatial information and in a user's ability to maneuver [93]. Kim et al. investigated the performance of FOV restriction in both the horizontal and vertical dimensions. This research found

that horizontal FOV restriction is more noticeable than vertical restriction, and this can consequently reduce immersion [94]. Panlener et al. investigated the impact of a restricted horizontal FOV in subjective median plane judgments and blind reaching tasks and found it negatively impacted distance judgments [95]. Adhanom et al. proposed a foveated FOV restriction, which uses an eye tracker that dynamically moves the center of the restrictor with the eye movements. The user study results showed that the most frequent area of focus of the participant's eyes was not in the center of the visual field, but rather in the lower region [96]. Eagle Flight for PlayStation 4 and PlayStation VR implemented an asymmetric FOV restriction which restricts the view in the opposite direction when turning while always keeping the middle of the bottom portion of the display unrestricted [97]. However, there is no study conducted to measure the performance of this method.

2.4.4 Limitations

Although restricting the field-of-view during movement is a common approach to mitigate cybersickness, some methods of FOV restriction have shown mixed results. Inappropriate design or implementation may introduce negative effects.

Some studies have shown that FOV restriction may increase user discomfort in certain applications. The FOV restriction is formed by a vignette around the peripheral of users' FOV. It was dynamically scaled based on users' velocity. However, improper occlusion of peripheral vision may expose the user to potential adverse effects, leading to more severe cybersickness [98]. Improperly displaying vignetting or increasing and decreasing vignetting too frequently can also lead to an increase in cybersickness symptoms [99].

The FOV restriction may impair subjective user experience. Previous experimental findings revealed a relationship between FOV restriction and the subjective sense of presence. A popular finding is that cybersickness has a negative relationship with a user's sense of presence [2]. In this light, FOV restriction

should improve the sense of presence, but some experiments have yielded the opposite conclusion [10, 100]. Conversely, some research has found that dynamic FOV restriction did not significantly affect presence compared to an unrestricted FOV [7, 42]. One potential reason for this discrepancy could be that the black mask/vignette added a sense of unreality to the virtual environment [7]. Research has also shown that FOV restriction can come at the cost of users' task performance in spatial learning [100].

The design principle of FOV restriction makes it reduce users' visibility. The restrictor symmetrically obscures the user's peripheral vision, depriving the user of a portion of the visual information that may be important for the user's activities in the virtual world, such as maintaining postural stability and discerning obstacle locations. Research has shown that a limited FOV can negatively impact distance estimation [101], postural equilibrium [102], and the user's control of orientation [103].

These studies confirmed that a certain degree of peripheral vision and an appropriate visible position should be maintained to both reduce the occurrence of cybersickness and provide a high-quality user experience.

Chapter 3

Passthrough FOV Restriction

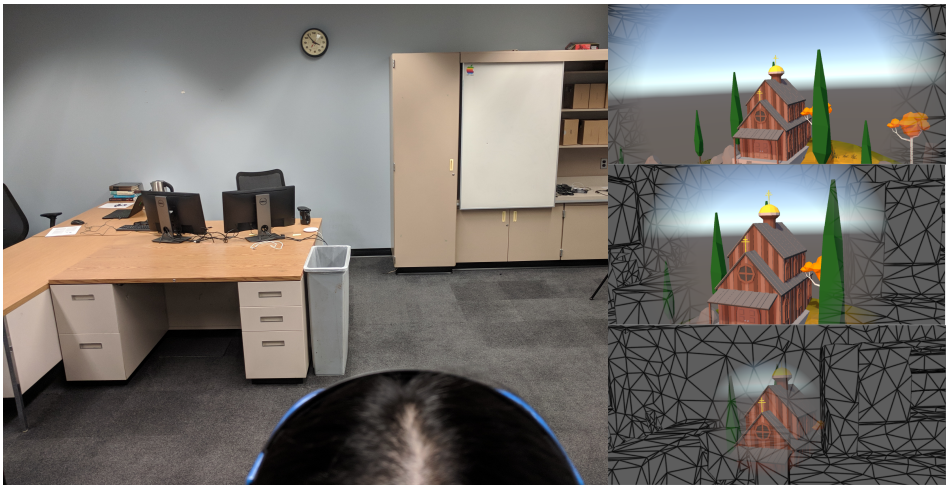

(a) (b)

Figure 3.1: (a) A virtual reality setup that allows the user to walk within a "room-scale" space bounded by the furniture and walls. (b) During movement, the displayed field of view of the virtual environment is dynamically reduced, revealing a wireframe 3D mesh of the physical environment. This provides a stable reference frame to mitigate motion sickness while simultaneously providing spatial cues that can help prevent collisions with real world obstacles.

3.1 Introduction

With the introduction of the HTC Vive, "room-scale" VR experiences became possible using consumer-level equipment. In these setups, natural walking is possible within the physical dimensions of a single room (e.g., 5m x 5m), resulting in a more comfortable user experience. However, most virtual environments are much larger than the available physical space, and so these applications commonly use a hybrid approach that combines both natural and virtual locomotion. This approach requires that the user maintain awareness of their locations in both the virtual environment and the real world simultaneously. Otherwise, the user may crash into physical obstacles such as walls or furniture. Furthermore, collisions may occur even when users are attempting to remain in the center of the room while primarily using virtual locomotion, because they will often"drift" when physically turning in place. As a result, virtual overlays, also known as "chaperones," are commonly displayed when the user approaches the boundaries of the physical space. While this can prevent a potential collision, their use is visually intrusive because they are overlayed on top of the virtual environment. Additionally, chaperones are generally represented as bounding boxes around an empty rectangular space, which does not correspond to the practical constraints of VR setups "in the wild," which may contain complex boundaries and interior obstacles.

We present a novel technique that attempts to address both motion sickness and physical collision avoidance simultaneously in "room-scale" VR setups that involve both virtual and physical locomotion. Similar to the approaches described previously, dynamic FOV modification is combined with the concept of rest frames. However, instead of an abstract virtual imagery in the periphery, we display a wireframe mesh that was generated from a 3D scan of the physical environment (see Figure 3.1). The user's viewpoint in the wireframe model retains a 1:1 mapping from the motion tracking system; no virtual locomotion is applied.

Therefore, users can experience the benefits of dynamic FOV modification (reduced motion sickness) while also maintaining awareness of their location in the physical world.

This approach is less intrusive than a virtual overlay, because the physical boundaries are only visible in the periphery during motion. The 3D model forms a earth referent which is stable relative to the Earth. The model will show up only when users get close to the obstacles. Some studies shows that the Earth referents benefit for maintaining postural stability [78] [104], especially when the referents are nearby [105]. Therefore, my technique is expected to efficiently reduce cybersickness by optimizing users postural stability. In the following sections, we describe the design and implementation of this technique and discuss opportunities for future research.

3.2 Technique Overview

My proof-of-concept prototype, shown in Figure 3.1, was tested using an Acer Windows Mixed Reality Headset. The software was implemented in Unity using VR Tunneling Pro, an open-source asset that provides several variations of dynamic field of view modification [106]. We modified the default "3D cage" functionality with a 3D mesh of the physical environment. To generate the custom model, we first used a Matterport professional camera to scan the labspace. Although the scanner can generate a high-quality scan with photorealistic textures, this level of detail was not necessary. In fact, a high-fidelity representation would likely negatively impact both system performance and the perceptual effectiveness of the visual effect due to dense optic flow in the peripheral regions. Instead, we found that a wireframe model with unlit, solid color triangular faces provided a more comfortable experience. Therefore, we removed the textures and used quadric edge collapse decimation to reduce the polygon count. The face color, line color, line width, and polygon count are all parameters that can be tuned. However, we found that 5,000 polygons yielded real-time framerates and visually

acceptable results for an approximately 6m x 9m room.

During the VR experience, the FOV restrictor can be displayed with a multitude of variations. The maximum amount of restriction, velocity mapping, and percentage overlap for the fade effect can be modified based on user preferences. In my current implementation, the FOV modification is activated based on either translational and angular velocity in the *virtual environment*. Additionally, the magnitude of restriction and the visibility of the physical environment model are coupled. However, it would also be useful to manipulate the visibility of the wireframe mesh based on physical movement in the *real world*, when collision avoidance is especially important. Furthermore, other weighting parameters, such as the distance to the boundaries and obstacles, could also be investigated. The visual appearance of the wireframe mesh (e.g., color, line thickness, etc.) could also be enhanced when a physical collision becomes increasingly imminent. As such, we are very interested in exploring the design space of these techniques more deeply in the future.

3.3 Discussion

This work presents an initial proof-of-concept that combines dynamic field of view modification with a rest frame representation of the physical environment geometry. In my implementation, the 3D scan of the lab space was conducted offline, and therefore the collision avoidance benefits will only apply to fixed obstacles and walls. However, inside-out tracking and environment mapping technologies are becomingly increasingly integrated with consumer virtual and augmented reality devices. We expect that it will be possible to implement the proposed technique in headsets with real-time 3D scanning capabilities in the foreseeable future, thereby introducing the possibility of dynamic obstacle avoidance. However, we believe it is still valuable to explore the design parameters and perceptual characteristics of these techniques despite the limitations of current-generation equipment.

Chapter 4

Ground-Visible Restriction

4.1 Introduction

Although restricting the field-of-view during movement is a common approach to mitigate cybersickness, it also reduces users' visibility of the virtual environment and can negatively impact their sense of presence [107, 108]. The standard implementation uses a symmetric circular mask to obscure the peripheral FOV, and may or may not include a semi-transparent buffer to smooth the edges of the restrictor. However, the effects of restricting different visual regions have not been sufficiently investigated; and asymmetric restrictors that separate the vertical, horizontal, binocular regions may provide a better cost-to-benefit tradeoff. For example, restricting the lower periphery where the ground plane is displayed may impact the user's postural stability or ability to maneuver around close obstacles, whereas restricting the upper periphery will only mask out portions of the skybox or ceiling.

The ground plane plays an important role in traverse. It is a metric for egocentric visual space that is used to perceive distance, estimate time-to-collision, and judge the relative size of objects. The optical flow of the observer translating relative to the ground plane can be used to compare spatial intervals [109]. A study in [110] shows that people would walk at a reduced speed and collide with

obstacles more frequently when the visibility window constrained vision to less than two-step lengths ahead when walking over complex terrain with irregularly spaced obstacles.

In a study of foveated FOV restriction, which uses an eye tracker to dynamically move the restrictor, results showed that the most frequent area of focus of the participant's eyes was not in the center of the visual field, but rather in the lower region [96]. This suggests that people subconsciously look downwards when walking, and supports the design decision to keep the ground plane visible during movement.

In this chapter, I propose and evaluate a novel variant of FOV restriction, which I refer to as the *ground-visible restrictor*. This technique uses an asymmetric mask that obscures the upper and side regions of the periphery, but leaves the lower region unoccluded. I then conducted a study to compare the ground-visible restrictor with the standard symmetric FOV restrictor during navigation through a complex maze-like virtual environment. My results showed that the ground-visible restrictor can improve user comfort during virtual locomotion, and also provides benefits for postural stability and subjective sense of presence. Furthermore, I did not observe any negative effects compared to the traditional symmetric restrictor, and I conclude that the ground-visible technique appears to be a generally superior form of FOV restriction. To the best of my knowledge, this is the first study about the effects of restricting different peripheral regions of the FOV on cybersickness.

4.2 Field-of-View Restrictor Design

The FOV restrictor was implemented in Unity using VR Tunneling Pro, an open-source asset that provides a computionally lightweight dynamic FOV restrictor that can be tuned using a variety of parameters [106]. The industry standard symmetric FOV restrictor was a straightforward use of this asset, as shown in the Figure 4.1(a). The user's view through each eye is obscured using a circular mask

with a black opaque texture in the periphery and a transparent circular hole in the center, and the edges of the opaque region can be optionally smoothed using a semi-transparent effect. The circular cutout is placed at a fixed distance from the center of projection and scales up and down based on the user's velocity, thereby increasing or decreasing the visible FOV.

FOV restrictors are typically displayed only when the participant is moving, and their size is dynamically scaled up to a defined outer radius, which determines how much of the screen is vignetted at maximum motion. An inner radius also defines the intermediate region that transitions linearly between 0 and full opacity. Although the implementation details vary in different applications, these parameters that are often tunable in VR game menus based on the users' preferences. I attempted to select parameters that were similar to those I observed in commercial games, and conducted internal pilot testing to verify that they provide a comfortable experience. In this experiment, I set the outer radius to 0.65 and the inner radius to 0.1. The speed of the dynamic scaling was set to 0.25 seconds from non-existence to appearance, or from existence to disappearance.

(a) (b)

Figure 4.1: (a) The standard FOV restriction technique uses a circular black mask to block the periphery of the visual field. (b) The ground-visible restrictor uses an asymmetric mask to preserve view of the lower periphery.

To create the ground-visible FOV restrictor, I modified the shader to generate

a custom texture mask. Instead of rendering the restrictor symmetrically, the horizontal and vertical effects were separated, and new variables were added to control the radius of the circular cutout in each direction. The bottom of the vertical effect was then effectively removed by setting the radius to be the maximum vertical FOV of the VR headset. All the other parameters remained consistent with symmetric restrictor. The ground-visible FOV restrictor is shown in the Figure 4.1(b).

4.3 User Study

4.3.1 Experiment Design

The effectiveness of the ground-visible restrictor was evaluated using a within-subjects design with the following three conditions:

- Symmetric restrictor (S)
- Ground-visible restrictor (GV)
- No FOV restriction (N)

In general, I hypothesized that the ground-visible restrictor would provide the overall best subjective experience for participants across a range of measures, including discomfort, visibility, and sense of presence, and would also exhibit quantitative differences in postural stability metrics derived from motion tracking. The specific measures and experimental hypotheses are described in more detail in sections 4.3.5 and 4.3.6.

The experiment was divided into three virtual reality sessions, one for each condition. Each session lasted 15-20 minutes and was conducted at least 24 hours after the previous session. This was necessary because cybersickness compounds over time and can potentially last for hours; it would therefore not be empirically valid to conduct all three conditions in a single session. The order in which each condition was distributed to participants was counterbalanced across the study.

This experiment was originally designed to be conducted in a tightly controlled lab setting. However, due to the COVID-19 pandemic, it was necessary to redesign the study for remote deployment over the internet. This introduced a number of logistical challenges to automate the experiment procedure and required specifically recruiting participants with existing access to consumer virtual reality equipment. The online study protocol was reviewed and approved by our University's Institutional Review Board (IRB).

4.3.2 Participants

Participants in this experiment were recruited through online postings on SteamVR online forums and Reddit interest groups. In the study, participants received study materials through emails and completed each session using their personal equipment. Participants were required to have normal or corrected-to-normal vision and be able to communicate in spoken and written English. Consent materials instructed participants that were pregnant or had a history of epilepsy or severe motion sickness not to participate due to safety concerns. Each participant was compensated with a $15 Amazon gift card upon completion of all three virtual reality sessions.

A total of 41 participants completed the study. The demographic questionnaire included separate questions with respect to biological sex and gender identity. In terms of biological sex, 38 participants self-identified as male, and only three participants reported as women. Due to prior findings of sex differences in motion sickness, my original study protocol had called for recruiting a balanced sample. However, I discovered that the number of women with access to virtual reality equipment at home remains a very small proportion of the population. This sampling bias is expected to be a major challenge for the virtual reality research community until it becomes possible to safely resume in-person human studies.

Participant ages ranged from 18 to 61 years old ($M = 30.5$, $SD = 9.1$). Two participants reported that they regularly play video games 0-3 hours per week,

eight reported 4-7 hours, 11 reported 8-11 hours, seven reported 12-15 hours, and 13 reported 16 or more hours per week. Although this would be expected when sampling from a population with access to their own VR equipment, it should be noted that this is a more experienced group than I typically see when recruiting from a university student pool or the general population.

Participants were using their own equipment because the study was conducted remotely due to the COVID-19 pandemic. The following headsets were used in the study: Valve Index (11), HTC Vive (7), HTC Vive Cosmos (1), Oculus Rift S (5), Oculus Rift (4), Oculus Quest with Link Cable (4), and Windows Mixed Reality (9). It should be noted that these devices do have varying technological characteristics such as refresh rate and field-of-view. Because the field-of-view restrictor is defined in screen space (as commonly implemented in commercial VR games), the visible field-of-view displayed using different headsets will vary. In a between-subjects experiment, this could potentially represent a confounding factor. However, the impact of technological differences on the experiment is mitigated by the within-subjects design. Because all participants experienced every experimental condition, I can still empirically compare the relative effects of no restriction, a moderate level of symmetric restriction, and ground-visible restriction, and technological differences between headsets cannot cause a spurious association between the independent and dependent variables.

4.3.3 Virtual Environment

The virtual environment (VE) was designed to be a maze that consists of complex pathways and turns, as shown in Figure 4.2. The maze was procedurally generated using an open-source Unity asset [111] and was consistent for all participants. A set of gold coins and red arrows were placed in the maze as waypoints to guide participants through the VE. This was done so that all participants followed the same paths through the maze, because individual exploration strategies would result in different locomotion behavior. Participants were instructed to follow

Figure 4.2: A partial overhead view of the virtual maze. The environment contains complex pathways and frequent turns. The locations of coins and arrows, which are used as waypoints, are indicated in gold and red.

the arrows and collect the gold coins, as shown in Figure 4.3. When a participant approached a coin, it would disappear, and the next one would appear in a readily visible location.

The participants navigated through the VE using a handheld controller. Virtual locomotion was achieved using view-directed steering, and participants turned using their physical body only. It should be noted that some VR controllers have analog sticks for velocity control, but others only have touchpads, and these input controls have different sensitivity profiles. Therefore, velocity was implemented at a constant rate of 2.5 meters per second. After extensive pilot testing, I determined that implementing smooth acceleration and deceleration over 0.25 seconds provided a good balance between comfort and responsiveness. Because the experimenter could not be physically present to direct the participant if they became lost in the maze, I implemented a function to teleport back to the last waypoint. This could be accessed via a spatial menu activated by the grip button on the

controller.

(a) (b)

Figure 4.3: (a) Participants traversed through the maze and collected gold coins. (b) Red arrows were displayed at crossroads to indicate the correct direction.

Participants were asked to rate their subjective discomfort at six checkpoints throughout the VR session. I adapted the same procedure from the original FOV restrictor study by Fernandes and Feiner [5], using the question "Please rate the discomfort level you are experiencing right now on a scale from 0 (not discomfort at all) to 10 (severe discomfort)." Responses were provided in the virtual environment using the graphical user interface shown in Figure 4.4. The participant was instructed to use a laser pointer attached to the controller to select their response, which I refer to as the discomfort score. After completing the checkpoint, the next path would be generated and the participant would be relocated to a different starting point in the maze.

The virtual environment was implemented in Unity 2018.3.6f1. The application used Steam VR was therefore compatible with multiple PC-tethered headsets. Although I could not control the equipment used by participants, the environment was designed to be computationally lightweight with low-poly art assets. During pilot testing using a variety of computers and VR setups, I observed framerates consistently above the headset refresh rate, including the Valve Index at 120hz.

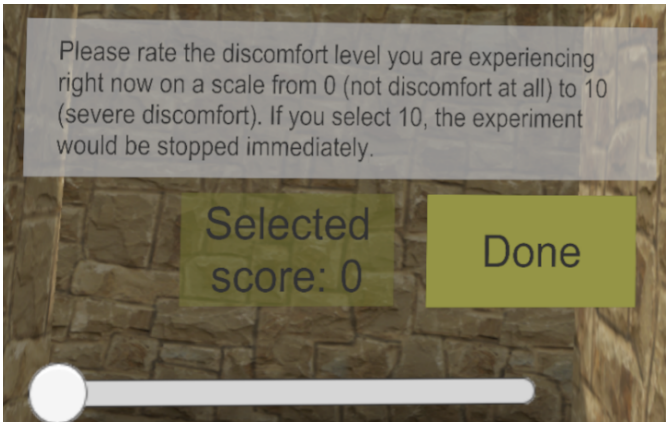

Figure 4.4: Participants selected a discomfort score using a spatial menu at multiple checkpoints throughout each VR session.

4.3.4 Procedures

Participants initially registered for the study through an online form and subsequently received an email containing the materials for the first session. In the first session, participants reviewed the information sheet and watched an instructional video that explained their tasks and demonstrated how to traverse through the VE using the controller. After starting the application, they completed the Kennedy-Lane Simulator Sickness Questionnaire (SSQ) [34] on their computer monitor using a keyboard and mouse. After completing the SSQ, the application instructed them to put on the headset and follow the instructions to start the virtual reality session.

Each session consisted of a pre-training trial and six experimental trials. Participants would first perform a short practice trial to ensure that they understood the control mechanisms of the virtual environment. Because the task was limited to just simple movement, and participants were already familiar with using their own VR equipment, the practice trial was brief and could be completed in approximately 30 seconds. After the practice trial, the experiment was started automatically. Each experimental trial required following the path through the maze as described in Section 4.3.3. This process was designed to last approximately two

minutes, although the actual completion time varied between participants. The start and end points for each of the six virtual paths were pre-defined and different for each trial, and the path order was determined pseudo-randomly.

At the end of each trial, participants encountered the checkpoint to capture their discomfort score. Participants were informed in advance that the session would be terminated if they reported a discomfort score of 10. They could also quite immediately by opening a menu with a controller button and selecting the "quit" option. They were also explicitly instructed in both the written and video materials to discontinue the session if they experienced motion sickness. Otherwise, the session would end automatically when the participant completed the final checkpoint.

Upon completing or terminating the VR session, the participants completed the SSQ post-test and a brief feedback questionnaire. In the third session, the participants also needed to complete a demographic questionnaire at the very end of the experiment. All data collected during the study were automatically compressed into a ZIP file. Participants submitted the data through a link in the email and waited for an email containing the materials for the next session or a gift card to be delivered 24 hours later.

4.3.5 Measures

Discomfort Scores. Similar to the procedure proposed by Fernandes and Feiner [5], I compute two dependent variables from the discomfort scores for each session: the participant's time-weighted *Average Discomfort Score (ADS)* and the *Relative Discomfort Score (RDS)*. I assume that the discomfort score was 0 at the beginning, and each reported score represents the degree of discomfort before the next checkpoint. The RDS is then computed using the following equation:

$$RDS = \frac{\sum\limits_{0 \le i \le t_{stop}} DS_i + (t_{max} - t_{stop} + 1) DS_{stop}}{t_{max}} \tag{4.1}$$

The value t_{max} represents the longest completion time of all participants. The completion time of each participant was t_{stop}. The discomfort score at t_{stop} was recorded as DS_{stop}. DS_i was the discomfort score at each second i prior to t_{stop}. If a participant terminated before t_{max}, their DS_{stop} was recorded as 10 and repeated each second from the terminated time until t_{max}. Similarly, if a participant finished early with a discomfort score less than 10, their final score was used as DS_{stop} and repeated.

Cybersickness. The responses on the Simulator Sickness Questionnaire (SSQ) were used to compute the overall SSQ score before and after each VR session. It should be noted that the SSQ and discomfort scores are not strictly redundant, as they are measuring distinct phenomena. While the SSQ reflects the magnitude of specific symptoms related to cybersickness, the discomfort score encompasses a broader scope that could include sensations not assessed by the SSQ. Additionally, to specifically identify motion sick participants, I also added the following yes/no question on the questionnaire, "Are you motion sick now?"

Subjective Experience. The feedback questionnaire included two sections regarding their experiences in the virtual environment. In the first part, participants were asked to rate their feeling for the three conditions using a 7-point Likert scale from 1="strongly disagree" to 7="strongly agree.":

1. I felt that my ability to see the virtual environment was restricted.
2. I had a sense of "being there" in the virtual environment.

For the purposes of readability, the responses for the first question were reversed so that higher ratings are associated with positive outcomes. I referred to these two criteria as *visibility* and *presence*, respectively. In the second section of this questionnaire, free-response questions were included to gather qualitative comments and suggestions.

Postural Stability. Movement data was recorded automatically by the VR application. During each frame, the system recorded the position and orientation of the participant in the VE, as well as the position and orientation of the participant's head in the physical world. I then computed several variability measures based on only the frames when the participant was moving virtually and the FOV restrictor would be visible. This was done by calculating the standard deviation of the physical movement deltas along a particular degree of freedom (x-axis, y-axis, roll rotation, and pitch rotation). I adapted these postural stability metrics from motion sickness literature in the field of kinesiology [22, 112]. For this experiment, I are particularly interested in pitch variability, because the differences between the restrictors could result in different head tilt behavior. If participants were compensating for reduced vertical visibility of the virtual environment when using the S restrictor, increased head tilt variability could contribute to visually-induced motion sickness.

Task Performance. The system also recorded the task completion time and the number of completed trials per participant.

4.3.6 Hypotheses

I formulated six scientific hypotheses regarding the dependent variables collected during this experiment:

- H1: Participants would report lower discomfort scores with the GV restrictor compared to the N and S restrictors.
- H2: Participants would report lower SSQ scores with the GV restrictor compared to the N and S restrictors.
- H3: Participants would report better visibility with the GV and N restrictors compared to the S restrictor.

- H4: Participants would report greater sense of presence with the GV and N conditions compared to the S restrictor.
- H5: Postural stability metrics would exhibit greater variability with the S restrictor compared to the GV and N restrictors.
- H6: Task performance measures would be superior with the GV and N restrictors compared to the S restrictor.

4.4 Results

Shapiro-Wilk tests of normality were conducted for all variables, and the results indicated that none of these data were normally distributed. Because my experiment was within-subjects and non-parametric, I applied the Friedman Rank Test to analyze differences between the three FOV conditions for each dependent variable. Descriptive statistics are therefore reported using median (Mdn) and interquartile range (IQR). All statistical tests used a significance value of $\alpha = 0.05$. When a Friedman Rank Test rejected the null hypothesis, I conducted post-hoc analysis using pairwise Conover tests with a Holm-Bonferroni correction for multiple comparisons. One participant had missing data due to accidentally uploading the wrong file, and was therefore excluded from the analysis.

Discomfort Scores. Results for the average and relative discomfort scores are shown in Figure 4.5. The analysis for ADS revealed significant differences among the three FOV conditions, $\chi^2(2) = 6.33$, $p = .04$. The GV restrictor ($Mdn = 0.35$, $IQR = 0.86$) was more comfortable than the N condition ($Mdn = 0.86$, $IQR = 1.92$), $p = .04$. However, ADS ratings for the S restrictor ($Mdn = 0.41$, $IQR = 1.56$) were not significantly different from the GV restrictor, $p = .36$, or N condition, $p = .36$. The analysis of RDS was also significant, $\chi^2(2) = 12.42$, $p = .002$. Post-hoc comparisons indicated that the GV restrictor ($Mdn = 0.44$, $IQR = 1.03$) was more comfortable than the N condition ($Mdn = 1.01$, $IQR =$

2.32), $p = .003$. The S condition ($Mdn = 0.69$, $IQR = 1.62$) was also more comfortable than N condition, $p = .03$. RDS ratings for the GV and S restrictors were not significantly different, $p = .33$. These results partially support hypothesis H1.

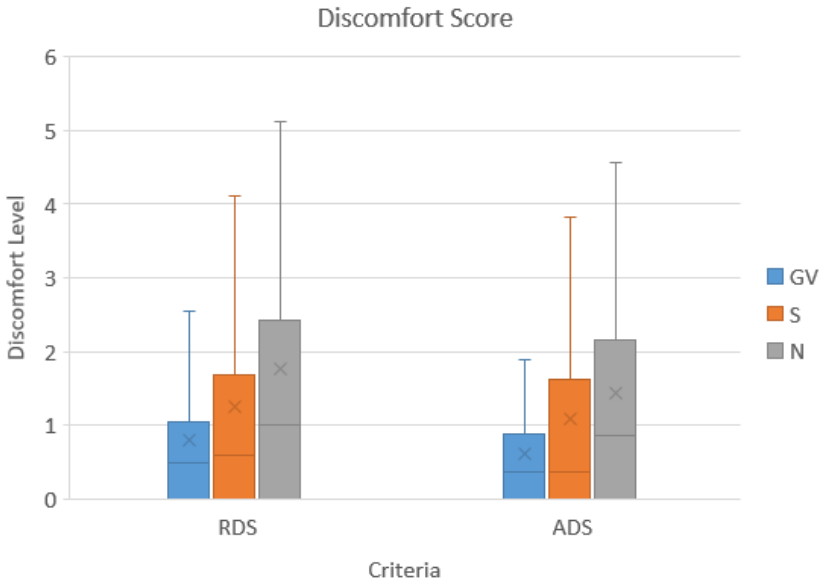

Figure 4.5: Box plots of the average discomfort score (ADS) and relative discomfort score (RDS) for each FOV condition. A value of 0 represents "no discomfort at all" and increasing numbers correspond to greater discomfort.

Cybersickness. Analysis of deltas between the pre- and post-SSQ scores did not indicate any significant differences among the three conditions, $\chi^2(2) = 1.77$, $p = .41$. Although I found no empirical support for hypothesis H2, SSQ scores were extremely low in all three conditions (see Table 4.1). Furthermore, participants reported motion sickness on the yes/no question in only 9 out of 120 trials. Taken together, these results suggest a floor effect.

Subjective Experience. Results from the feedback questionnaire are shown in Figure 4.6. The analysis of visibility ratings revealed a significant difference among

Table 4.1: SSQ Scores and Completion Times

Condition	Mdn SSQ (IQR)	Mdn Completion Time (IQR)
N	7.48 (22.44)	784.35 sec. (130.22)
S	7.48 (14.96)	750.72 sec. (89.37)
GV	7.48 (15.90)	747.60 sec. (89.56)

the three FOV conditions, $\chi^2(2) = 58.23$, $p < .001$. The N condition ($Mdn = 6$, $IQR = 3$) was given favorable visibility ratings compared to the S restrictor ($Mdn = 1$, $IQR = 1$), $p < .001$, and the GV restrictor ($Mdn = 2$, $IQR = 2$), $p < .001$. However, there was no significant difference observed between the GV and S restrictors, $p = .12$. These results partially support hypothesis H3.

The analysis of presence ratings was also significant, $\chi^2(2) = 27.37$, $p < .001$. Participants reported a greater sense of presence in the N condition ($Mdn = 6$, $IQR = 1.75$) compared to both the S restrictor ($Mdn = 5$, $IQR = 3.75$), $p < .001$, and GV restrictor ($Mdn = 5$, $IQR = 2.75$), $p = .002$. However, presence ratings for the GV restrictor were also significantly higher than the S restrictor, $p = .05$, thereby fully supporting hypothesis H4.

Postural Stability. Analysis of pitch variability was significant, $\chi^2(2) = 8.40$, $p = .02$. Participants exhibited greater pitch variability when using the S restrictor ($Mdn = 0.16$, $IQR = 0.08$) compared to the GV restrictor ($Mdn = 0.14$, $IQR = 0.06$), $p = .02$. The N condition ($Mdn = 0.14$, $IQR = 0.07$) was not significantly different from either the S restrictor, $p = .08$, or the GV restrictor, $p = .29$. Analysis of x-axis variability was also significant, $\chi^2(2) = 6.91$, $p = .03$. Participants exhibited greater side-to-side motion variability when using the S restrictor ($Mdn = 0.00131$, $IQR = 0.00053$) compared to the GV restrictor ($Mdn = 0.00130$, $IQR = 0.00053$), $p = .03$. The N condition ($Mdn = 0.00136$, $IQR = 0.00057$) was not significantly different from either the S restrictor, $p = .39$, or the GV restrictor, $p = .39$. The analysis for z-axis variability was not significant, $\chi^2(2) = 5.20$, $p = .07$, nor was roll variability, $\chi^2(2) = 1.60$, $p = .45$.

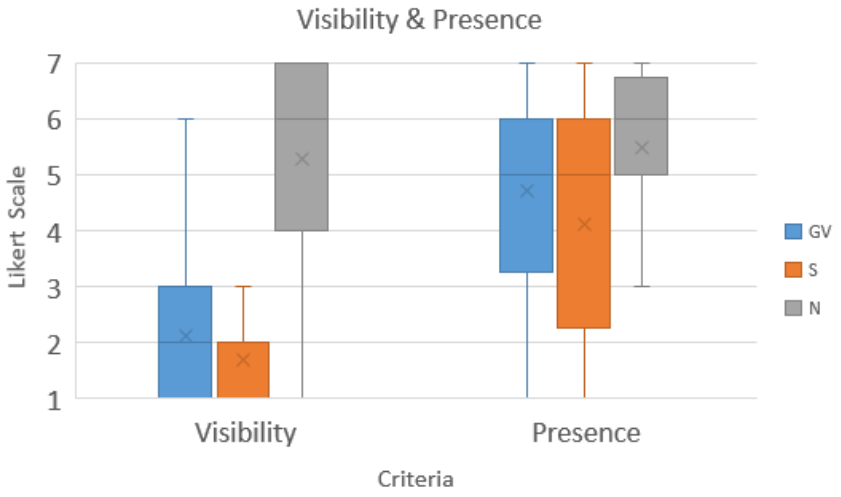

Figure 4.6: Box plots of visibility and sense of presence ratings for each session. The direction of the scale was adjusted so that higher values are associated with positive outcomes.

These results partially support hypothesis H5.

Task Performance. Only one participant stopped a VR session early; all others fully completed the six trials in all three conditions. This outlier was therefore excluded from the analysis. Median completion times for each condition are shown in Table 4.1. The test did not reveal any significant differences among the three conditions, $\chi^2(2) = 1.95$, $p = .37$. I therefore did not find any empirical support for hypothesis H6.

4.5 Discussion

Participants reported the lowest levels of discomfort when using the GV restrictor, as measured through both average and relative discomfort scores. The GV restrictor was the only intervention that was significantly improved comfort compared to the condition without restriction. Although the discomfort scores reported when using the GV and S restrictors were not significantly different, my results suggest

that the keeping the ground visible does not appear to reduce the efficacy of FOV restrictors.

SSQ scores were extremely low overall, which was surprising for a 15-20 minute VR experience that uses locomotion. These results, along with the very sparse self-reports of motion sickness, suggest a floor effect, and it was unlikely that the restrictors had any opportunity to further reduce cybersickness. I therefore cannot make any definitive conclusions regarding the effects of GV restriction on symptoms specific to motion sickness. There are several possible explanations for unusually low cybersickness levels in this experiment. Chief among them is the sampling bias inherent in recruiting online participants with pre-existing access to VR equipment. Generally speaking, participants are early adopters, and it stands to reason that people who are more prone to cybersickness would be less likely to invest in a VR setup for personal use. It should also be noted that this population was heavily dominated by men, and I were able to recruit very few women for this study. This is unfortunate due to previous findings that have suggested women are more susceptible to motion sickness compared to men [22]. These issues are very difficult to address during the COVID-19 pandemic, and I plan to conduct follow-up studies that sample from a wider population after it becomes safe to resume in-person experiments.

To my knowledge, the effects of FOV restriction on postural stability have not been previously evaluated, and this analysis is an additional source of novelty in this experiment. The increased pitch rotation variability when using the S restrictor was likely caused by the need to compensate for reduced vertical visibility. The lower region of the periphery provides perceptual cues that are valuable for close quarters maneuvering, and participants may have needed to tilt their head up and down more often to see imagery that was readily visible when using the GV restrictor. Additionally, the S restrictor also produced an increase in side-to-side positional variability, which is indicative of postural sway, despite the fact that the left and right regions of the periphery were the same as the GV restrictor. These results suggest that the keeping the ground visible during FOV restriction

facilitates stability in control of the body.

It is unsurprising that the condition without restriction was rated highest by participants for both environment visibility and sense of presence. Although the original study by Fernandes and Feiner did not find any significant differences in presence, it should be noted that their experiment used a more conservative FOV restrictor that was designed to be imperceptible to the user [5]. In contrast, I modeled my restrictor design more similarly to implementations commonly present in commercial VR applications such as Skyrim VR or Google Earth VR. In this context, it is notable that the GV restrictor provides benefits for sense of presence compared to S restrictor. Although the visibility score for the GV restrictor was also generally higher, these subjective ratings exhibit a high degree of variability that prevents us from making any definitive scientific conclusions.

Although I had hypothesized that the different conditions would influence navigation task performance, no significant effects were found for completion times. The sampled population, which primarily consisted of experienced users, should again be considered when interpreting these results. I suspect that FOV restriction could have a greater impact on task performance for users that are less familiar with navigation using virtual reality controllers or for people that have greater susceptibility to motion sickness. Therefore, I still consider this to be an interesting question to revisit in future studies.

It is also valuable to consider how the virtual environment design may have influenced the results. In the free response questions, some participants mentioned that the S restrictor sometimes blocked part of the gold coins and red arrows, which led them to stop more often to increase their visibility of the virtual environment. The GV restrictor reduces this problem, which makes it more useful for environments that require close quarters maneuvering. However, for large open environments with objects at a distance, the GV restrictor would have fewer opportunities to provide an advantage. That said, I have not observed any negative effects from using the GV restrictor compared to the S restrictor, and given the potential advantages, I conclude that it appears to be a generally superior

technique.

Finally, as in any study, the scope and generalizability is limited by the specific parameters tested in the experiment. FOV restrictors inherently require a tradeoff between comfort and other aspects of the subjective experience, and the ideal balance is different for every user. In VR applications intended for practical use, I believe that parameters such as restrictor size and speed should be customizable based on the users' individual preferences and tolerances for virtual locomotion.

4.6 Conclusion

In this chapter, I proposed and evaluated ground-visible FOV restriction, a novel form of a widely used technique for mitigating cybersickness in virtual reality. I conducted a within-subjects user study across three separate sessions that compared the proposed method with a traditional symmetric restrictor and a control condition without FOV restriction. The results showed that the ground-visible restrictor offers potential benefits for user comfort, postural stability, and subjective sense of presence. I found no evidence of potential drawbacks to keeping the ground visible during FOV restriction. I therefore conclude that this form appears to be superior to symmetric restrictors when navigating through environments with a visible ground plane. However, this experiment specifically focused on existing VR headset owners, and further study would be needed to generalize these results to naive users or the overall population.

Chapter 5

Side Restriction

5.1 Introduction

Virtual rotation can cause significant discomfort. In the prior work, I made the intentional decision to only study virtual forwards or backward translation in the experiment. However, virtual rotation is an important component in commercial VR games and could induce severe cybersickness. Many commercial VR games avoid continuous virtual rotation and instead it by "snap turn" techniques. Much prior research has also implemented FOV restriction during virtual rotation.

FOV restriction shows promise for reducing the severe cybersickness resulting from head rotation, with vection and optokinetic nystagmus (OKN) being the main triggers [26]. In virtual rotational movements, the effect of OKN is very small, consequently strong vection would be the main cause of cybersickness. Vection, as a visually induced sense of self-motion, would be elicited by wide FOV. At the same time, virtual rotation also brings a large amount of optical flow, which is one of the causes of cybersickness. Therefore, a moderate restriction of the FOV in the virtual rotation should help to reduce cybersickness.

A symmetric restrictor impedes the user's peripheral vision during locomotion, which becomes more important while executing a virtual rotation. During walking or turning, eye movements and the line of sight will generally be aligned

with the end of the desired path [113]. Therefore, during turning, users' sight lines would be aimed in the direction of the turn, but the symmetric restrictor would partially obscure sight lines in this area. An asymmetric restrictor could potentially compensate for this limitation by accommodating the lateral offset in the user's line of sight. However, to the best of my knowledge, no studies have been conducted to evaluate the effectiveness of asymmetric side restriction during virtual turns.

In this chapter, I introduce and evaluate a novel variant of FOV restriction, referred to as the *side restrictor*, which preserves perceptual cues in the user's peripheral vision towards the direction of turns. My primary goal is to explore the effects of left and right peripheral FOV restriction during rotation. I propose that this asymmetric FOV implementation would be more appropriate during virtual turns and could be combined with other forms of asymmetric restriction during translation. To evaluate these technique, I conducted a virtual reality user study with a between-subjects design (N=93) that compared the side restrictor with the traditional symmetric FOV restrictor and an unrestricted FOV as a baseline. Participants completed a navigation task in a complex maze-like virtual environment that required frequent virtual turns using a handheld controller. My results showed that the side restrictor was effective in mitigating cybersickness and reducing discomfort during virtual locomotion. The proposed technique also provided benefits for subjective visibility and enabled users to remain immersed in the virtual environment for longer periods of time. Furthermore, in my study, I did not observe any negative effects compared to the traditional symmetric restrictor, and I therefore conclude that side restriction appears to be a superior design choice for virtual environments with frequent virtual turns.

The most similar technique to my proposed method was implemented in Eagle Flight, a video game developed by Ubisoft for the Playstation VR platform. The game implements an asymmetric FOV restrictor that limits the user's FOV in the direction *towards* the turn when flying in open space, which seems counterintuitive. They also restricted the user's FOV symmetrically when flying in a confined

space, such as tunnels.

In contrast, my method was designed for navigating virtual environments on the ground, which requires turning around corners and avoiding collisions with near-field obstacles. Regardless, to my knowledge, there have not been any empirical studies that have evaluated the efficacy of asymmetric side FOV restriction.

5.2 Field-of-View Restrictor Design

(a) symmetric restrictor (b) side restrictors (left and right turns)

Figure 5.1: (a) The standard symmetric FOV restriction technique uses a circular black mask to occlude the periphery. (b) When the user turns to the left or right, an asymmetric mask is used to restrict the FOV on the side opposite to the turn, and the center is shifted laterally into the turn.

To implement the FOV restrictors, I extended VR Tunneling Pro, an open-source asset for the Unity game engine. This package provides a computationally lightweight restrictor using a symmetric circular mask that can be customized using a variety of parameters [106]. The mask is defined by an outer radius and an inner radius, as shown in Figure 5.1(a). The range beyond the outer radius was completely obscured, while the region between the inner and outer radius provided a smooth transition from transparent to opaque. By default, the shader implemented in VR Tunneling Pro defines the mask radii in screen space. I modified this shader to compute the size of restriction according to the degrees

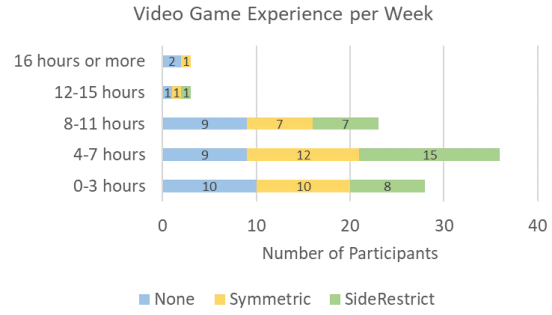

(a)

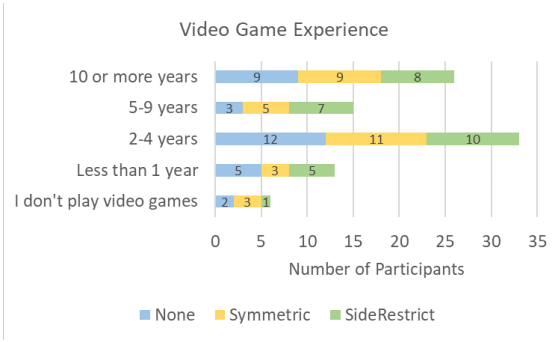

(b)

Figure 5.2: (a) The number of hours per week of video game experience for participants. (b) The number of years of participants' video game experience. Gaming experience was approximately balanced between the three conditions.

of FOV so that my results could be more easily interpreted and implemented on various headsets.

The FOV restrictor was displayed only when the participant was moving virtually and was not visible when they were physically walking. The restrictor size was dynamically scaled from the maximum FOV to a defined minimum degree. I attempted to select parameters that were similar to those I observed in commercial games and validated their performance in providing a comfortable experience through internal pilot testing. In this experiment, I set the outer FOV to 60 degrees and the inner FOV to 59 degrees. The size of the fully opaque region was comparable to the parameters used in Wu et al. [13], although the intermediate

region was smaller. The dynamic scaling of the FOV mask was applied over a duration of 0.25 seconds when participants started or stopped moving.

Symmetric FOV Restrictor Design. The symmetric FOV restrictor was generated by aligning the angle between the camera's view direction and the vector formed by any point on the edge of the black opaque texture to the center of the camera and, as shown in Figure 5.1(a). The symmetric restrictor was activated whenever the user initiated either a virtual turn or a forward/backward translation.

Side FOV Restrictor Design. To create the side FOV restrictor, I modified the shader to separate the horizontal and vertical FOV, and a new variable was added to control the restricted side in the horizontal direction. All the other parameters remained consistent with the symmetric restrictor. The logic was as follows:

- If the user moves virtually forward or backwards, the FOV is restricted symmetrically.
- If the user turns virtually to the left or right, or virtually moves forward/backwards and physically turns left or right, the FOV is restricted only on the side *opposite* to the turn direction. The restrictor in the turning direction is stretched so that the leftmost or rightmost point is positioned at infinity, and the view on the side into the turn remains visible. The center also shifts laterally in the direction of the turn.
- If the user stops moving virtually, the FOV is unrestricted.

The lateral shift of the side restrictor was synchronized with the user's virtual turning. To determine parameters, I conducted internal pilot testing with a Vive Pro Eye. Users navigated through the same virtual environment used in my study without FOV restriction, and I computed the average angular shift of the users'

eyes during virtual turns. Based on these data, I set the lateral shift of the side restrictor to ±17 degrees. Examples of the side restrictor during virtual turns are shown in Figure 5.1(b).

5.3 User Study

5.3.1 Experiment Design

To evaluate the effectiveness of side restriction during virtual turns, I conducted a between-subjects study with the three conditions:

- No restriction (baseline)
- Symmetric restriction
- Side restriction

In general, I hypothesized that the side restrictor would provide benefits across a range of subjective measures, including cybersickness, discomfort, sense of presence, and visibility of the virtual environment. I also hypothesized that participants would stay immersed in the virtual environment for a longer period of time when using the side restrictor. My specific measures and scientific hypotheses are described in more detail in sections 5.4 and 5.5.

Due to the COVID-19 pandemic, the study was designed for remote deployment over the internet and required explicit recruitment of participants with existing access to consumer virtual reality equipment. All experimental procedures and tutorials were fully automated. To provide a consistent experience, the VR headsets were limited to an Oculus Quest or Quest 2, and the virtual environment was deployed directly to the participant's device. Running in PC-tethered mode using Oculus Link was not supported. The online study protocol was reviewed and approved by the University's Institutional Review Board (IRB).

5.3.2 Participants

Participants were recruited through online postings on interest groups of Reddit, Facebook, and Linkedin. They were required to have access to an Oculus Quest or Quest 2 and be prepared to sideload an application on the device. Study materials and video tutorials were provided through email along with an APK file of the application. Participants were required to have a normal or corrected-to-normal vision and be able to communicate in spoken and written English. Participants that were pregnant or had a history of epilepsy or severe motion sickness were instructed not to participate due to safety concerns. Each participant was compensated with a $10 Amazon gift card upon submitting the post-questionnaire and uploading a log file recorded by the headset.

A total of 93 participants completed the study, of whom 60 identified themselves as male and 33 identified themselves as female. I managed the distribution of VR application during the study so that the biological sex was evenly balanced across the three conditions. Participant ages ranged from 18 to 55 years old ($M = 23.30$, $SD = 5.95$). A total of 84 participants used an Oculus Quest 2. Only 9 participants used a Oculus Quest 1 and were divided among the three conditions. Upon review of the automatically captured logs in the questionnaire submission system, I discovered that 69 of the participants completed the study from the same IP address. However, thorough review of the data files and quantitative and qualitative questionnaires responses indicated that all the submissions were authentic data from different people. I were able to determine that these participants had completed the study at a large supermall with a VR arcade. Therefore, it appears that approximately two-thirds of my participants were sampled from a more general population than VR headset owners. This diversity is also reflected in the self-reports of video game experience. As shown in the Figure 5.2, participants had a wide variety of video game experience, including novice and infrequent gamers. Furthermore, the distribution of gaming experience across the three conditions was approximately balanced.

(a) (b)

Figure 5.3: (a) A partial overhead view of the virtual maze, which contains complex pathways and frequent turns. The waypoints that defined a linear path are indicated in gold. (b) To complete the task, participants collected the gold coins by traveling over them.

5.3.3 Virtual Environment

The virtual environment was procedurally generated using QMaze, an open-source Unity asset [111]. The 10x10 meter maze contained frequent turns so that I could explore the performance of side FOV restriction during virtual rotations (see Figure 5.3(a)). The width of each passageway was approximately 1.5 meters. The virtual environment was consistent for all participants. Gold coins were placed in a linear path throughout the maze, and participants were instructed to collect them by walking over them (see Figure 5.3(b)). These waypoints guided participants through the virtual environment so that they followed a consistent path.

Participants were instructed to stand during the virtual reality experience and only turn virtually without physically rotating their bodies. Locomotion was implemented using view-directed steering, which was controlled via the thumbstick on an Oculus Touch controller. The parameters for velocity and acceleration were determined through extensive pilot testing to determine a good balance between comfort and responsiveness. The maximum translational velocity was 2.5

meters per second, and the maximum rotational velocity was 45 degrees per second. When participants moved the thumbstick forward or backwards, translation would accelerate or decelerate smoothly over 0.25 seconds until the maximum was reached. Rotational acceleration was implemented similarly over a time window of 0.5 seconds. If the participant became lost or disoriented, they could press the grip button on the controller to open a spatial menu and teleport back to the last waypoint.

The virtual environment was implemented in Unity 2019.4.29f1. To ensure good performance on the Oculus Quest, the assets used to create the maze comprised computationally lightweight, low-poly models. During pilot testing, I measured the framerate on the Quest and observed that it was able to stay approximately equal to the device's maximum refresh rate of 72hz. I also the data files from each participant and verified that the virtual experience was rendered at the appropriate framerate.

5.3.4 Procedure

Upon viewing the advertisement, participants registered for the study online. The instructions and study materials were then distributed to each participant via email. Participants reviewed the information sheet and watched an instructional video that explained the task and controls. After watching the tutorial, the instructions walked them through the steps of sideloading the application on the Oculus Quest. The participants then could put on the headset and follow the in-game instructions to start the study.

Once immersed in the virtual environment, participants completed the Kennedy-Lane Simulator Sickness Questionnaire (SSQ) [34] that was displayed on a large spatial menu. They used the controller to point and select responses on the graphical user interface. After completing the SSQ, participants completed a 30-second practice trial to familiarize themselves with moving in the virtual environment. When they were ready to continue, they were prompted to select a button that

would begin the experiment. Participants then completed 20 experimental trials that required following a path through the maze defined by the gold coins, as described in Section 5.3.3. Each trial was a different path that was designed to last approximately two minutes, although the actual time varied between participants. The paths were manually created to be equivalent in length and number of turns, and the path order for each participant was determined pseudo-randomly.

At the end of each trial, participants reached a checkpoint and were instructed to rate their subjective discomfort on a spatial menu using a controller (see Figure 5.4). The question "Please rate the discomfort level you are experiencing right now on a scale from 0 (no discomfort at all) to 10 (severe discomfort)" was adapted from the original FOV restrictor study by Fernandes and Feiner [5], which has also been used in Wu et al. [13]. Participants were instructed at the beginning that the navigation task would be stopped without penalty if they reported a discomfort score of 10. Participants were also able to quit immediately via a spatial menu that was opened using the controllers grip button. The written and video materials both instructed participants to discontinue the study if they felt motion sick, and they would still be compensated for participating. Otherwise, the navigation task ended upon reaching the final checkpoint. The experiment lasted approximately 40 minutes.

Upon completing or terminating the navigation task, participants filled out the SSQ post-test in the virtual environment. They were then instructed to remove the headset, connect it to their computer, and retrieve the log file generated by the application. Participants uploaded this data file and completed a feedback post-questionnaire and demographic questionnaire using Qualtrics.

5.4 Measures

I evaluated the performance of the three FOV restrictors using the following metrics.

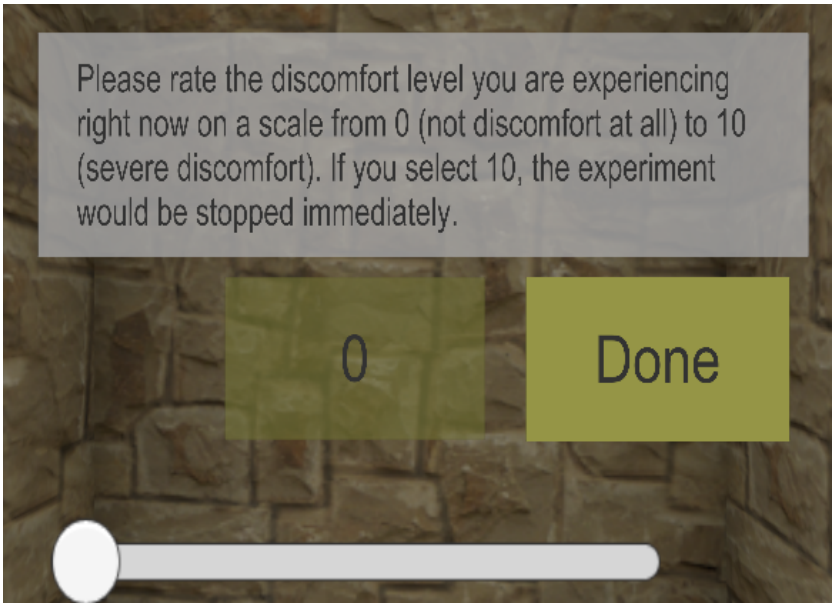

Figure 5.4: Participants used a spatial menu to rate their discomfort on a 0-10 scale at checkpoints throughout the experimental task.

Cybersickness. The responses on the Simulator Sickness Questionnaire (SSQ) were used to compute the overall SSQ score before and after completing the navigation task. Because I had no a priority hypotheses about specific symptoms, the SSQ subscales were not analyzed separately. Additionally, it should be noted that the SSQ assesses the magnitude of symptoms related to cybersickness, which is more specific than general discomfort ratings at checkpoints during the study.

Discomfort Scores. Two dependent variables were calculated from the discomfort scores for each condition following the metrics proposed by Fernandes and Feiner [5]: the participant's time-weighted *Average Discomfort Score (ADS)* and the *Relative Discomfort Score (RDS)*. The ADS measured the mean discomfort score from the time participants entered the VE to the time they left. The ADS may be a good way to measure subjective discomfort if participants complete all trials in the experiment. However, due to the duration my experiment, most participants terminated the navigation task early, so it may not be the best way

to measure participants' relative performance. For example, two participants may complete the experiment with the same ADS, but one participant may spend more time in the VE before finishing. The RDS takes into account the time spent in the VE and measured the average discomfort score using the following equation:

$$RDS = \frac{\sum_{0 \leq i \leq t_{stop}} DS_i + (t_{max} - t_{stop} + 1) DS_{stop}}{t_{max}} \tag{5.1}$$

The value t_{max} represents the longest duration of all participants. The duration of each participant was t_{stop}. The discomfort score at t_{stop} was recorded as DS_{stop}. DS_i was the discomfort score at each second i prior to t_{stop}. If a participant terminated before t_{max}, their DS_{stop} was recorded as 10 and repeated each second from the terminated time until t_{max}. If a participant finished early with a discomfort score less than 10, their final score was used as DS_{stop} and repeated.

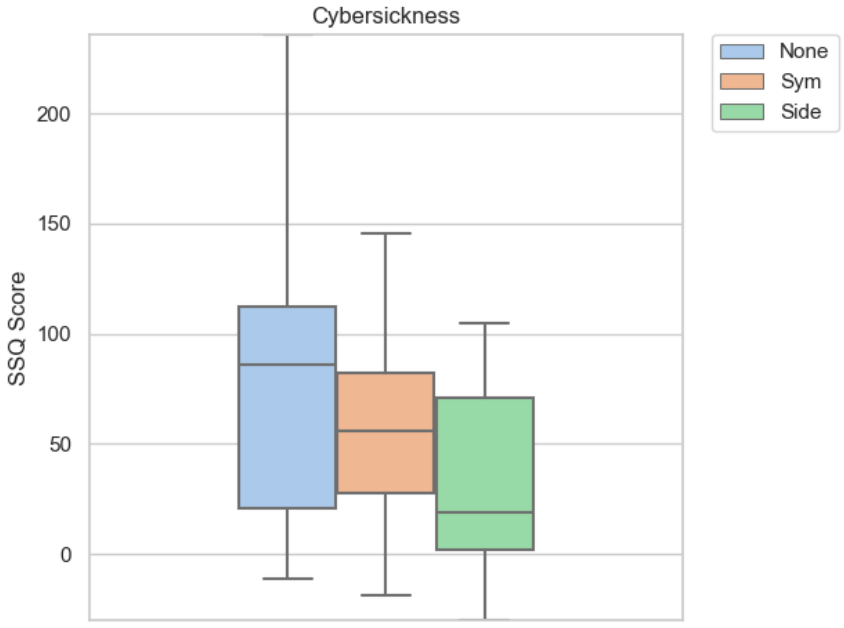

Figure 5.5: Box plots of the delta SSQ scores for each condition. Users reported significantly lower cybersickness when using the Side restrictor compared to the None condition.

Objective Measures. Because the navigation task terminated when the participant felt motion sick or entered a discomfort score of 10, the amount of time spent in the virtual environment is also a useful objective measure. The system therefore recorded the time starting from the beginning of the first experiment trial until the participant completed or quit the task, as well as the total number of completed trials for each participant.

Subjective Experience. The feedback post-questionnaire asked participants to rate agreement with the following two statements on a 7-point Likert scale:

1. It was difficult to see the virtual environment while turning.
2. I had a sense of being present in the virtual environment.

The responses for the first question were reversed so that higher ratings are associated with positive outcomes for both variables. In my results, I refer to these two measures as *visibility* and *presence*, respectively. Free-response questions were included to gather qualitative feedback.

5.5 Hypothesis

I formulated five scientific hypotheses regarding the dependent variables collected during this experiment:

- H1: Participants would report lower delta SSQ scores with the side restrictor compared to the baseline and symmetric restrictors.
- H2: Participants would report lower discomfort scores with the side restrictor compared to the baseline and symmetric restrictors.
- H3: Participants would be immersed in the navigation task longer with the side restrictor and symmetric restrictor compared to the baseline.

- H4: Participants would report better visibility with the side restrictors and baseline compared to the symmetric restrictor.
- H5: Participants would report a greater sense of presence with the side restrictor and baseline compared to the symmetric restrictor.

5.6 Results

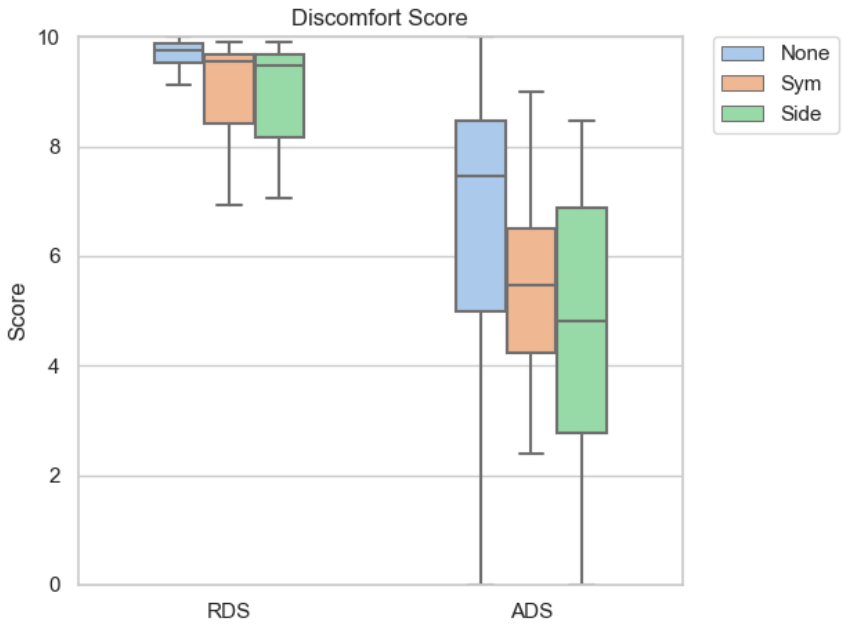

Figure 5.6: Box plots of average discomfort scores (ADS) and relative discomfort scores (RDS) for each condition. A value of 0 represents "no discomfort at all" and increasing numbers correspond to greater discomfort. Users reported significantly lower ADS and RDS when using the Side restrictor compared to the None condition.

Shapiro-Wilk Normality tests were conducted for all variables, and the results indicated that only the duration data was normally distributed and rest of these data were not normally distributed. For the non-parametric data, I applied the

Kruskal-Wallis H test to analyze differences between the three FOV restrictor conditions (None, Symmetric, and Side) and reported descriptive statistics as median (Mdn) and interquartile range (IQR). All statistical tests used a significance value of $\alpha = 0.05$. When a Kruskal-Wallis H test rejected the null hypothesis, I conducted the post-hoc analysis using pairwise Conover tests with a Holm-Bonferroni correction for multiple comparisons.

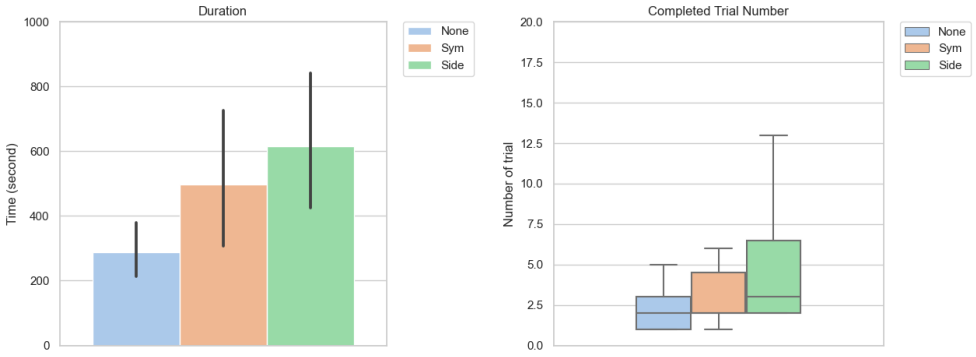

(a) (b)

Figure 5.7: (a) Bar charts showing mean and standard deviation of immersion duration for each condition. (b) Box plots of number of completed trials for each condition. Participants using the Side restrictor persisted significantly longer in the virtual environment and completed a greater number of trials compared to the None condition.

Cybersickness. Cybersickness results are shown in Figure 5.5. Analysis of deltas between the pre- and post-SSQ scores indicated significant differences among the three conditions, $\chi^2(2) = 9.73$, $p = .008$. Post-hoc comparisons revealed that the Side restrictor ($Mdn = 18.70$, $IQR = 69.19$) had significantly lower SSQ score compared to the None condition ($Mdn = 86.02$, $IQR = 91.63$), $p = .006$. However, the Symmetric restrictor ($Mdn = 56.10$, $IQR = 54.23$) was not significantly different from either the Side restrictor, $p = .07$, or the None condition, $p = .29$. These results partially support hypothesis H1.

Discomfort Scores. Results for the average and relative discomfort scores are shown in Figure 5.6. The analysis for ADS revealed significant differences among the three FOV conditions, $\chi^2(2) = 9.67$, $p = .008$. Post-hoc comparisons found that the Side restrictor ($Mdn = 4.81$, $IQR = 4.11$) was more comfortable than the None condition ($Mdn = 7.46$, $IQR = 3.47$), $p = .006$. ADS ratings for the Symmetric restrictor ($Mdn = 5.46$, $IQR = 2.28$) were also significantly more comfortable than the None condition, $p = .04$. However, the Symmetric and Side restrictors were not significantly different, $p = .42$.

The analysis of RDS was also significant, $\chi^2(2) = 12.92$, $p = .002$. Post-hoc comparisons indicated that the Side restrictor ($Mdn = 9.49$, $IQR = 1.50$) was significantly more comfortable than the None condition ($Mdn = 9.75$, $IQR = 0.35$), $p = .001$. The Symmetric condition ($Mdn = 9.55$, $IQR = 1.25$) was also more comfortable than None condition, $p = .010$. RDS ratings for the Side and Symmetric restrictors were not significantly different, $p = .44$. These results partially support hypothesis H2.

Objective Measures. Results for task duration and number of completed trials are shown in Figure 5.7. For the time data, 6 extreme outliers greater than 2 standard deviations from the mean were excluded to avoid biasing the analysis (1 in None, 2 in Side, and 3 in Symmetric). The trimmed data were then analyzed using a between-subjects ANOVA, which revealed significant differences among the three conditions, $F(2) = 3.57$, $p = .03$, $\eta^2 = .08$. Participants in the Side restrictor condition ($M = 615.06$, $SD = 583.21$) remained immersed in the navigation task significantly longer than the None condition ($M = 288.11$, $SD = 243.60$), $p = .03$. However, the Symmetric restrictor ($Mean = 497.92$, $SD = 538.62$) was not significantly different from either the Side restrictor, $p = .62$, or the None condition, $p = .22$.

The analysis of the number of completed trials also revealed significant differences among the three conditions, $\chi^2(2) = 9.53$, $p = .009$. Participants in the Side restrictor condition completed significantly more trials ($Mdn = 3$, $IQR = 4.5$)

compared to the None condition ($Mdn = 2$, $IQR = 2$), $p = 0.005$. Similar to above, the Symmetric condition ($Mdn = 2$, $IQR = 2.5$) was not significantly different from either the Side restrictor, $p = .15$, or the None condition, $p = .16$. Taken together, these results partially support hypothesis H3.

Subjective Experience. Results from the feedback questionnaire are shown in Figure 5.8. The analysis of visibility ratings revealed a significant difference among the three FOV conditions, $\chi^2(2) = 20.54$, $p < .001$. Post-hoc analysis indicated that the Side restrictor ($Mdn = 6$, $IQR = 4.5$) was given favorable visibility ratings compared to the Symmetric restrictor, $p = .002$. The None condition ($Mdn = 6$, $IQR = 2.5$) was also associated with higher visibility compared to the Symmetric restrictor ($Mdn = 2$, $IQR = 3.5$), $p < .001$. However, there was no significant difference observed between the Side restrictor and the None condition, $p = .62$. These results support hypothesis H4.

The analysis of presence ratings was not significant among the three conditions, $\chi^2(2) = 1.74$, $p = .418$. Participants reported similar sense of presence in the None condition ($Mdn = 5$, $IQR = 3.0$), the Symmetric restrictor ($Mdn = 5$, $IQR = 3.5$), and the Side restrictor ($Mdn = 5$, $IQR = 2.0$). I therefore did not find any empirical support for hypothesis H5.

5.7 Discussion

5.7.1 Effects on Cybersickness and Discomfort

The side restrictor was the only technique that significantly reduced the level of cybersickness compared to the unrestricted condition. This is strong evidence supporting the side restrictor as a viable method for mitigating cybersickness during virtual turns.

The non-significant results for the symmetric restrictor are consistent with the original study by Fernandes and Feiner [5]. Their primary findings involved

subjective discomfort ratings, and SSQ scores were also not significantly different between restrictor conditions. Responses to my open-ended questions revealed potential explanations for the underperformance of the symmetric restrictor.

Because the virtual environment was a maze with many turns, participants needed to make a lot of virtual rotations during navigation. Some participants reported that when making a turn, the symmetric restrictor occluded their view of the maze in the turning direction. To avoid hitting the maze wall and to correctly follow the path, they had to stop frequently and wait for the restrictor to disappear before continuing. This sporadic turning process, as well as the appearance and fading of the restrictor, was likely to induce strong optical flow. This, in turn, could have increased the level of cybersickness. Conversely, the side restrictor gave participants a clear view of the path while turning, allowing them to complete the turn smoothly without pausing.

The side restrictor was rated as significantly more comfortable than the unrestricted condition, which provides further support that this implementation improves users' experience during virtual turns. Although there was not a significant difference between the side restrictor and the symmetric restrictor, the side restrictor had the lower median value, which suggests that the lateral shift of the restrictor center did not cause any additional discomfort.

5.7.2 Effects on Subjective Experience

Visibility when using the side restrictor was rated significantly higher than when using the symmetric restrictor. This confirms that the proposed technique effectively increases visibility for users during turns, and subsequently enhances their awareness of the environment in the direction of the turn. This makes the experience more convenient for the user and can improve safety during virtual turns. Additionally, visibility ratings for the side restrictor were very close to those of the unrestricted control condition; there was no significant difference between the two. This suggests that the side restrictor more effectively compensates for the

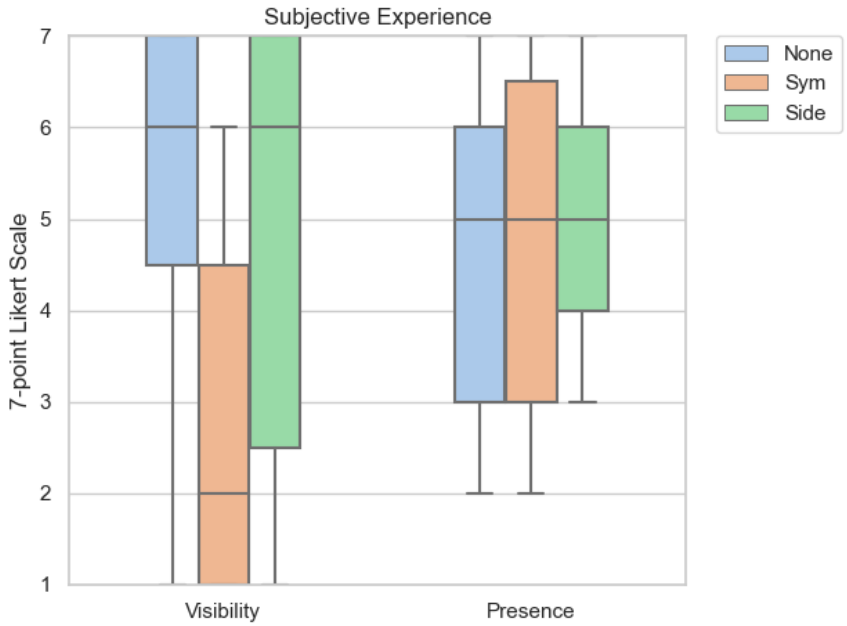

Figure 5.8: Box plots of visibility and sense of presence ratings for each condition. The direction of the scale was adjusted so that higher values are associated with positive outcomes. Users reported significantly worse visibility when using the Symmetric restrictor compared to the Side and None conditions.

shortcomings of the traditional symmetric implementation and provides visibility during virtual turns that is comparable to an unrestricted experience.

The ratings for the sense of presence were very close among all three conditions. The results of various previous studies also show a mixed relationship between presence and FOV restriction. Presence has a positive relationship with vection [7], but a negative relationship with cybersickness level [2]. Since the use of a restrictor typically results in a reduction of both vection and cybersickness, it is not surprising that the trade-off between the changes of vection and cybersickness had a minimal effect on presence. A similar phenomenon can also be seen in previous studies [5, 7].

5.7.3 Effects on Objective Measures

Participants using the side restrictor remained immersed for significantly longer and completed a greater number of trials compared to those in the unrestricted condition. According to some questionnaire responses, being unable to see the surroundings while turning in the symmetric condition induced enough frustration to lead them to stop the experiment. Because participants were explicitly instructed to discontinue if they felt motion sick, and the task ended immediately upon a discomfort score of 10, the longer immersion time provides further evidence that the side restrictor was more effective in mitigating negative effects. Furthermore, the fact that participants also completed more trials when using the side restrictor indicates that the longer duration was not due to navigating the maze more slowly.

5.7.4 Limitations

This study has some practical limitations that may have influenced its results. All participants were recruited online, and the experiment was conducted remotely due to the COVID-19 pandemic. However, the variety and complexity of the logs captured during the experiment, in addition to the varied responses to the open-ended questions, supports the authenticity of the data. In any remote study, potential differences in the physical environments of the participants could have influenced their performance. However, these outside factors are also generally present for actual users "in the wild" who would also be experiencing VR in different physical environments. Thus, my experimental results should be generalizable to the real-world conditions in which FOV restriction techniques would be used. However, it should be noted that this study tested a specific type of virtual experience, and evaluation of FOV restriction in a wider range of VR experiences remains an open question for future work.

The vast majority of participants used a Quest 2, which has minor differences in field-of-view and resolution compared to the original Quest. Given the very

small proportion of Quest 1 participants in each condition, I believe that these differences between devices are unlikely to have any meaningful impact on the results. Additionally, I relied on participants following the headset's built-in instructions for adjusting the interpupillary distance. Additional variability could have been introduced if some participants did not adjust it correctly, which is a limitation of conducting studies remotely.

5.8 Conclusion

In this chapter, I proposed and evaluated asymmetric side FOV restriction, a new variant of a widely used technique for mitigating cybersickness in virtual reality. I conducted a between-subjects user study with three conditions to compare the proposed technique with a traditional symmetric restrictor and a control condition without FOV restriction. My results showed that the side restrictor maintains similar outstanding benefits for improving user comfort compared to the symmetric restriction, while providing better performance for cybersickness reduction, visibility, and immersion time during virtual times. At the same time, I found no evidence of potential drawbacks to applying side restriction. Therefore, I conclude that this form of asymmetric FOV restriction appears to be superior to symmetric restriction during virtual rotation. It performs particularly well in close environments involving a large number of turns. Although I required participants to have access to the Oculus Quest, based on my information about participants, they were distributed across experience levels, and a large proportion of them had minimal experience with video games. Therefore, my study results are not solely limited to experienced VR users, despite the remote modality.

Chapter 6

Adaptive Restriction

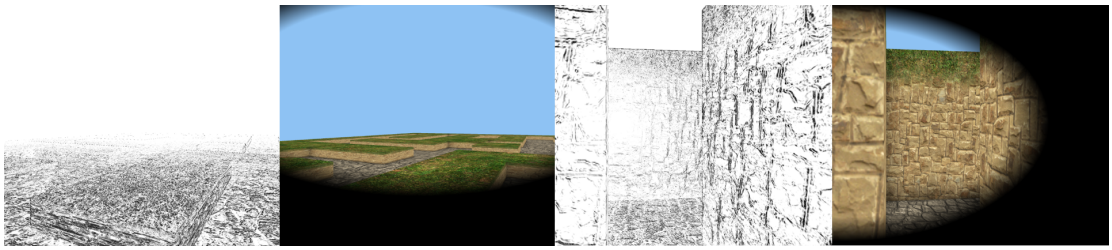

Figure 6.1: The adaptive restrictor is designed as a dynamic asymmetric mask to restrict the field-of-view in higher optical-flow regions when the user moves virtually. The two grayscale images show the optical flow patterns from wide open and close-quarter virtual environments, respectively. The color images show how the adaptive restrictor dynamically responds to occlude the regions with the most optical flow.

6.1 Introduction

Virtual locomotion - the act of moving in virtual environments - is a fundamental interaction task in VR. However, The optical flow generated by locomotion can induce cybersickness in VR, especially when the user is only moving virtually, but not physically. The optical flow of imagery across the visual field is strongly

associated with cybersickness and is a contributing factor to vection, which is the sensation of illusory self-motion in the absence of physical movement [1]. The optical flow patterns in wide field-of-view displays can produce severe vection [17] that is inconsistent with the motion sensed by the vestibular system. Consequently, strong optical flow generated by virtual locomotion is often considered a major cause of cybersickness and could be further exacerbated by a wide field-of-view. Field-of-view (FOV) plays an important role in perceiving optical flow. Studies have shown that motion at the periphery of the FOV is likely to produce more vection than motion at the center of the FOV [114].

Existing widely used implementations of FOV restriction often use a symmetric solid color or static mask to block the user's peripheral FOV [5]. However, this may result in sub-optimal occlusion of peripheral vision, and the vignette of the restrictor may expose the user to unnecessary optical flow. Moreover, the commonly used implementation is triggered by the user's forward and/or angular velocity, regardless of whether the optical flow in a scene is low or high. Reducing the FOV in scenes with minimal optical flow may not be necessary and could negatively impact the user's performance. An asymmetric restrictor that takes into consideration the amount of optical flow in different parts of the virtual scene to block only the regions of the virtual scene with the highest optical flow could overcome this limitation. To the best of my knowledge, no prior studies have been conducted to evaluate the effectiveness of asymmetric FOV restriction that dynamically adapts based on optical flow during virtual locomotion.

In this chapter, I introduce *adaptive field-of-view restriction*, a novel technique that responds dynamically based on real-time assessment of the optical flow generated by movement through a virtual environment. I propose that adaptive FOV restriction provides a more flexible implementation for use in a wider variety of situations ranging from wide open spaces to close-quarter environments. To evaluate this technique, I conducted a user study in which participants completed in a navigation task in two different virtual scenes using controller-based locomotion. The experiment compared the adaptive restrictor, standard symmetric restrictor,

and an unrestricted control condition in two different virtual scenes that generate drastically different optical flow patterns. The results showed that the adaptive restrictor was effective in reducing both cybersickness and subjective discomfort while obscuring less of the field-of-view, thereby allowing users to have better visibility and sense of presence compared to the symmetric restrictor.

6.2 Field-of-View Restrictor Design

6.2.1 Symmetric FOV Restrictor Design

The symmetric FOV restrictor was implemented by extending VR Tunneling Pro, an open-source asset for the Unity game engine [106]. This framework provides a computationally lightweight restrictor using a symmetric circular mask that can be customized using a variety of parameters. The mask is defined by an outer radius and an inner radius, as shown in Figure 6.2. The peripheral FOV beyond the outer radius was completely obscured by a black opaque mask, while the region between the inner and outer radius provided a smooth transition from transparent to opaque similar to a feathering effect. I modified the default method of measuring the mask radius in screen space to angular FOV so that my results could be more easily interpreted and consistently implemented on various headsets.

The symmetric restrictor was activated whenever the user initiated either a virtual translation or rotation. When the movement conditions are met, the size of the restrictor was dynamically scaled from the maximum FOV to a preset minimum degree. I selected parameters that were similar to those used in widely used commercial applications and validated their performance in providing a comfortable experience through internal pilot testing. In this experiment, the outer radius of the FOV restrictor was set to 60° and the inner radius was set to 55°. The FOV restrictor was dynamically scaled over a duration of 0.25 seconds when participants started or stopped moving.

Figure 6.2: The standard symmetric FOV restriction technique uses a circular black mask to occlude the periphery. The inner and outer radii define the region in which the mask gradually transitions from fully transparent to fully opaque.

6.2.2 Adaptive FOV Restrictor Design

An overview of the adaptive restrictor pipeline is shown in Figure 6.3, and a more detailed description is provided in Algorithm 6.2.2. Similar to the standard symmetric restrictor, adaptive restriction was invoked during virtual locomotion and was not displayed when users were physically moving only. The optical flow was measured once per frame, and the FOV parameters were dynamically smoothed over a time window of 0.5 seconds. The parameters in each step were selected based on their performance in pilot testing so that they provide a comfortable experience to the user.

The algorithm defines the following variables: c, a 2D vector (c_x, c_y), representing the center of the restrictor in the x and y direction; r, a 2D vector (r_x, r_y) representing the radius in x and y direction; c_{offset}, a 4D vector (c_{offset_u}, c_{offset_d},

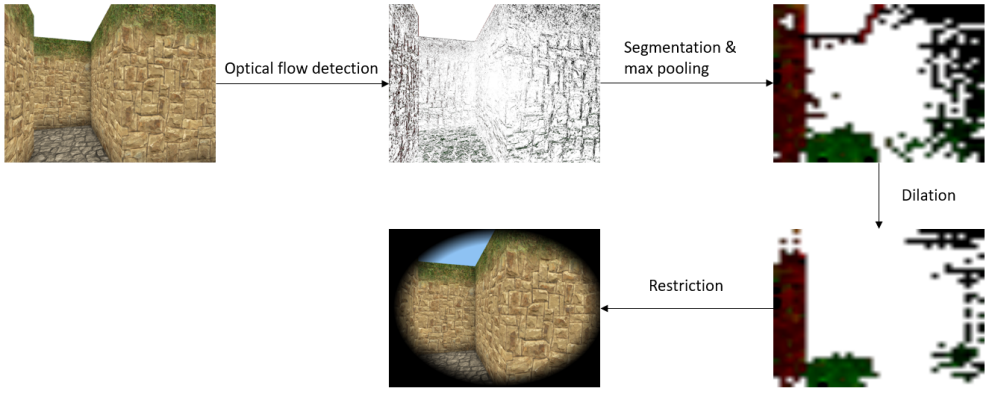

Figure 6.3: The adaptive field-of-view restrictor is designed as an asymmetric mask that occludes the FOV in high optical-flow regions when the user moves virtually. Based on the image rendered to the screen, per-pixel optical flow is measured in real-time and pooled in a 32×32 grid. Image processing techniques are then used to detect regions of high optical flow and the size and shape of the FOV restrictor is adjusted dynamically.

c_{offset_l}, c_{offset_r}), representing center offset in up, down, left and right directions; r_{min}, a 2D vector (r_{min_x}, r_{min_y}), representing the minimum restrictor radius in x and y directions; c_{screen}, a 2D vector (c_{screen_x},c_{screen_y}), representing the screen center. The function $Clamp(value, min, max)$ clamped the given value between the minimum value and maximum value, and w was a weight variable. I applied $w = 1$ in my implementation.

The input for optical flow detection were images of the viewpoint generated based on the view and projection matrices of the monoscopic virtual camera. The threshold in step 4 was determined through pilot testing with multiple users to ensure that the region of maximum optical flow can be selected and that the restrictor would not block too much of the user's vision. Subsequent pilot testing was also conducted to confirm that the selected parameters provide a comfortable user experience. To avoid jitter, we also applied a smoothing process to both the center and the radius of the restrictor. Additionally, to avoid cases where the restrictor center would be too heavily offset towards the boundary, resulting in a very small viewing area, we added steps 15-25 to adjust the minimum radius of

the restrictor by the maximum offset of its center. The larger the center offset, the larger the minimum radius; conversely, the smaller the center offset, the smaller the minimum radius.

6.3 User Study

6.3.1 Experiment Design

In the experiment, the goal was to evaluate and compare the effectiveness of three different FOV restriction conditions (no restriction, symmetric restriction, adaptive restriction) in two different virtual scenes (close-quarter and open environments). The study used a mixed design with FOV restriction as a within-subjects variable and virtual scene as a between-subjects variable. Participants experienced the FOV restrictors in separate VR sessions, each of which was separated by at least 24 hours to avoid the compounding effects of cybersickness. The order of within-subjects trials was counterbalanced using a Latin Square design. For the virtual scenes, participants were divided into two groups, one experiencing the close-quarter environment and the rest experiencing the open environment. The number of male and female participants was balanced across the two groups.

This experiment was conducted in my laboratory. The study protocol was reviewed and approved by our University's Institutional Review Board (IRB).

6.3.2 Participants

Participants were recruited through the university. They were required to have a normal or corrected-to-normal vision and be able to communicate in spoken and written English. Participants that were pregnant or had a history of epilepsy or severe motion sickness were instructed not to participate due to safety concerns. Each participant was compensated with a $20 Amazon gift card upon finishing all three sessions.

(a) (b)

Figure 6.4: (a) A partial overhead view of the virtual maze, which contains complex pathways and frequent turns. (b) To complete the task, participants collected the gold coins by traveling over them.

A total of 38 participants completed the study, of whom 19 identified themselves as male and 19 identified themselves as female. Participant ages ranged from 19 to 27 years old ($M = 22$, $SD = 2.46$) with a wide variety of video game experience, ranging from very little to over 10 years of gaming experience.

6.3.3 Equipment

Participants experienced the virtual environment using a Vive Pro Eye Headset and Valve Index controllers. The headset provides a stereoscopic view with a resolution of 1440 $\times$ 1600 per eye, a refresh rate of 90Hz, and a field-of-view of approximately 110°. The experiment was run on an Intel Core i7-7820HK 2.90GHz PC running Windows 10 Home with 16 GB of RAM and an NVIDIA GeForce GTX 1080 graphics card. The virtual environment was implemented in Unity 2019.4.29f1. During the study, I recorded the frame rate on the Vive Pro Eye for each participant and observed that it was able to stay approximately equal to the device's maximum refresh rate of 90hz.

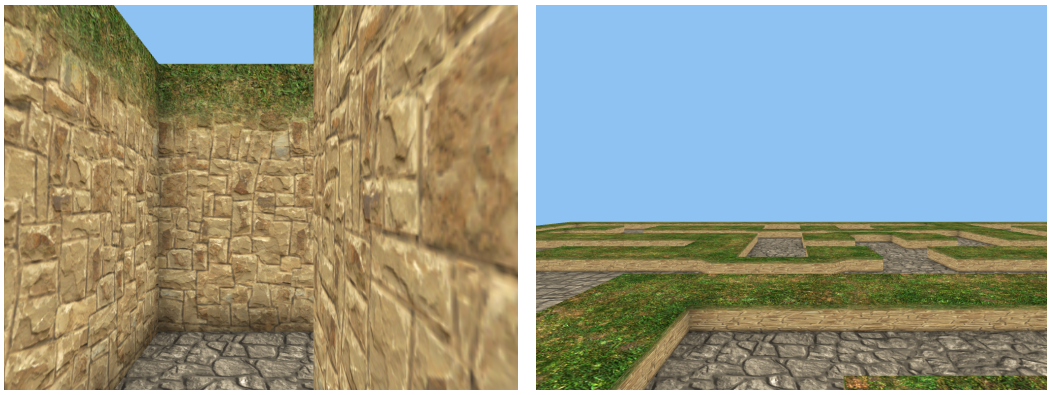

(a) (b)

Figure 6.5: Screenshots of the close-quarter (a) and open environments (b). The layout of both scenes was consistent and only differed in wall height, which resulted in drastically different optical flow patterns from similar virtual paths.

6.3.4 Virtual Environment

Two virtual environments contained a 10x10 maze generated using QMaze, an open-source Unity asset [111]. Both mazes contained the same complex tunnels and frequent turns. The width of each tunnel was approximately 1.5 meters (see Figure 6.4). Gold coins were placed in a linear path throughout the maze, and participants were instructed to walk through them. These coins guided participants through the virtual environment so that they followed a consistent path. The wall height was the only difference between the two environments. The close-quarter environment had 3 meters high walls, and the open environment had 0.15 meter high walls (see Figure 6.5) .

6.3.5 Procedure

Because cybersickness can potentially persist for hours after exposure [16], participants came to my lab for three separate sessions separated by at least 24 hours. At the beginning of the first session, participants read the information sheet, were instructed on the task, and learned how to use the controller. Afterwards, they

immersed themselves in the virtual environment and completed the Simulator Sickness Questionnaire (SSQ) [34]. After filling in the questionnaire, each participant would then perform a short practice trial to ensure that they understood the control mechanisms of the virtual environment. The practice trial was expected to take about 30 seconds.

Participants were instructed to stand during the virtual reality experience. They were able to virtually move forward/backward and turn virtually via the thumbstick on a Valve Index controller using view-directed steering. Forward velocity was 2.5 meters per second, and angular velocity was 45° per second. The velocity parameters were constant and determined through extensive pilot testing to determine a good balance between comfort and responsiveness. Participants were also able to physically rotate their heads, but were instructed not to walk physically.

After the practice trial finished, participants then completed 10 experimental trials, each of which was designed to take approximately two minutes, resulting in an overall immersion time of about 20 minutes. Participants were required to follow a path through the maze defined by the gold coins, as described in Section 6.3.4. At the end of each trial, participants reached a checkpoint and were instructed to rate their subjective discomfort level on a scale from 0 to 10 (see Figure 6.6), following a similar procedure to the seminal FOV restrictor study by Fernandes and Feiner [5]. Participants were instructed at the beginning that the navigation task would be stopped immediately if they reported a discomfort score of 10. Participants were also able to quit immediately via a spatial menu that was opened using the controller's grip button.

During each trial, the virtual reality application collected information, including discomfort score for each trial, position and orientation data for each frame, the overall task duration, the number of completed trials, and the size of the displayed FOV. Upon completing or terminating the navigation task, the participants completed the SSQ post-test and a feedback questionnaire. At the end of

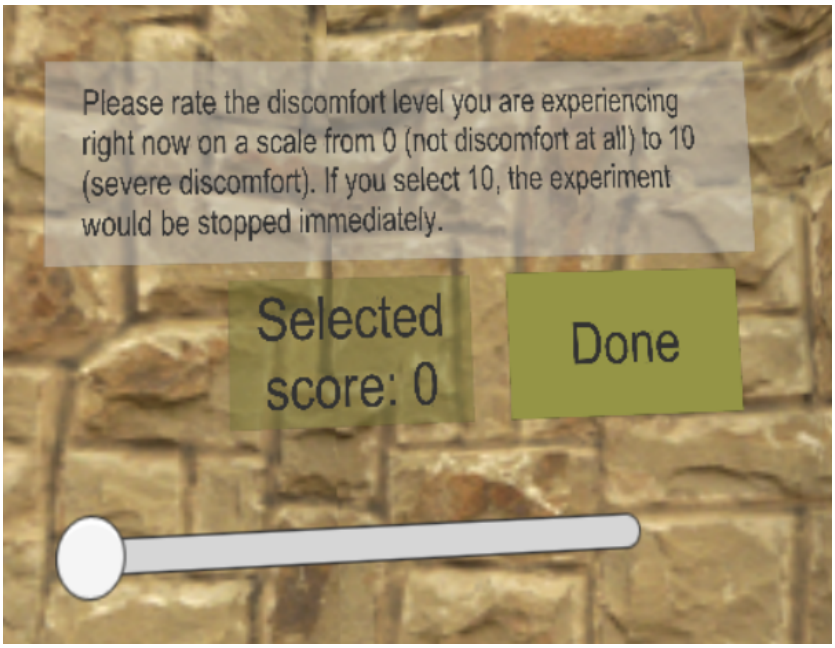

Figure 6.6: Participants used a spatial menu to rate their discomfort level on a 0-10 scale at checkpoints throughout the experimental task.

the third session, the participants also needed to complete a demographic questionnaire. Each session was designed to take approximately 25 - 30 minutes to complete all procedures, including pre- and post-questionnaires.

6.4 Measures

The performance of the three FOV restriction conditions was evaluated using the following metrics.

Cybersickness. The Simulator Sickness Questionnaire (SSQ) scores were calculated using the deltas between participants' responses to the SSQ before and after each session of the study. This is a standard questionnaire to assess the extent of each symptom associated with cybersickness.

Discomfort Scores. I adopted the metrics proposed by Fernandes and Feiner [5] to process the discomfort score and calculate two variables: the participant's time-weighted *Average Discomfort Score (ADS)* and the *Relative Discomfort Score (RDS)*.

$$RDS = \frac{\sum_{0 \leq i \leq t_{stop}} DS_i + (t_{max} - t_{stop} + 1) DS_{stop}}{t_{max}} \tag{6.1}$$

$$ADS = \frac{\sum_{0 \leq i \leq t_{stop}} DS_i}{N} \tag{6.2}$$

The amount of time each participant immersed in the virtual environment was t_{stop}. The longest one was t_{max}. The discomfort score at t_{stop} was recorded as DS_{stop}. DS_i was the discomfort score at each second i prior to t_{stop}. If a participant terminated before t_{max}, their DS_{stop} was recorded as 10 and repeated each second from the terminated time until t_{max}. If a participant finished early with a discomfort score less than 10, their final score was used as DS_{stop} and repeated. N was the number of trials completed. This two metrics rated the participants' general level of discomfort rather than specific symptoms, and are therefore a distinct, yet complementary, measure from the SSQ scores.

Task Performance. The task was terminated immediately if the participant selected a discomfort level of 10 or used the button to quit the game. Thus, the overall immersion time in the virtual environment could be expected to be an objective indicator of cybersickness to some extent. The duration, defined as the time from when the participant enters the first trial to the completion or exit of the game, and the number of completed trials were automatically recorded by the system. In addition, although the velocity and angular velocity were constant during the navigation task, participants would stop more frequently to take a break if they had stronger cybersickness. Therefore, the average time they spent

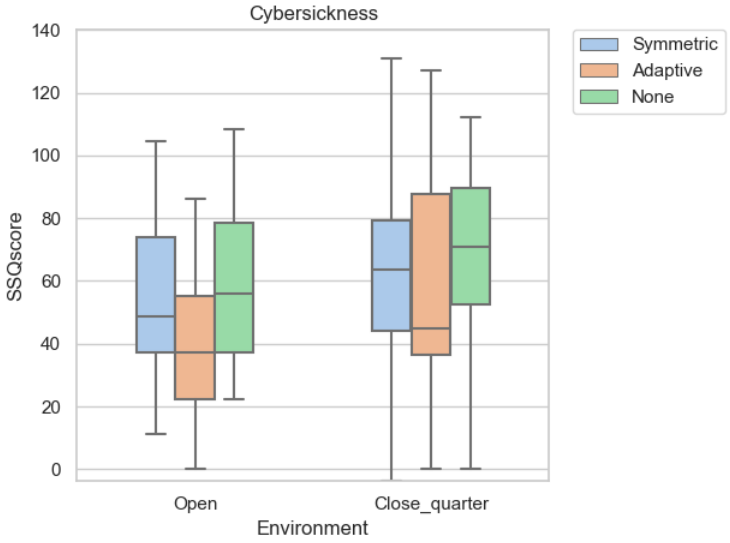

Figure 6.7: Box plots of the delta SSQ scores for each condition. Users reported significantly lower delta SSQ score when using the Adaptive restrictor compared to the None condition.

in each trial was calculated using the following equation:

$$\text{average time per trial} = \frac{\text{total duration}}{\text{number of completed trials}} \tag{6.3}$$

Only data from participants who completed at least one trial were used to calculate the average time per trial.

Subjective Experience. The feedback questionnaire asked participants to rate their agreement with the following two statements on a 7-point Likert scale:

1. It was difficult to see the virtual environment during locomotion.

2. I had a sense of being present in the virtual environment.

The first measure was referred to as *visibility*, and its score was reversed so that higher scores are associated with positive findings. The second measure was referred to as *presence* in the results. It should be noted that I only used a single

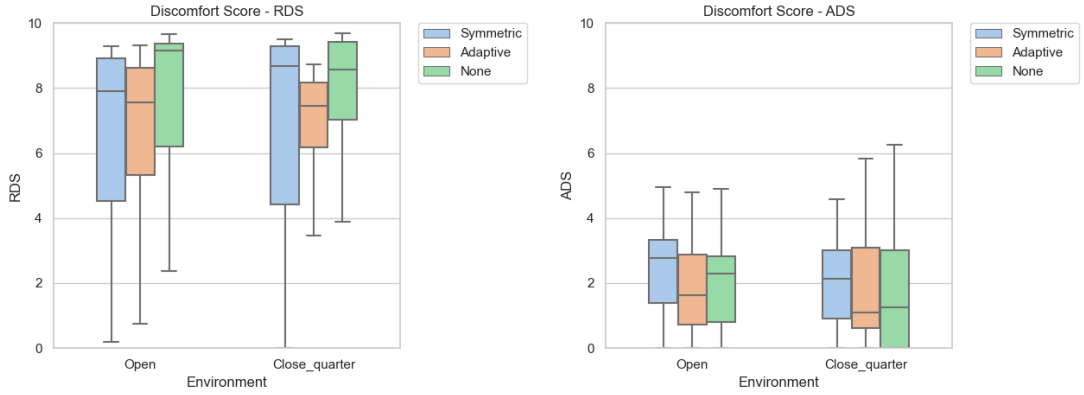

(a) (b)

Figure 6.8: (a) Box plots of relative discomfort scores (RDS) for each condition per environment. (b) Box plots of average discomfort scores (ADS) for each condition per environment. A value of 0 represents "no discomfort at all" and increasing numbers correspond to greater discomfort. Users reported significantly lower RDS when using the Adaptive restrictor and Symmetric restrictor compared to the None condition.

question to assess presence instead of a longer format questionnaire because this was only a tertiary measure and I were concerned with limiting overall participation to less than 90 minutes across the three sessions.

6.5 Hypotheses

Symmetric FOV restriction has been shown to effectively reduce discomfort, but this simplistic implementation may result in over-restriction that negatively impacts other aspects of the subjective user experience. Our goal in developing the adaptive restrictor, therefore, was to provide a superior benefits with less severe tradeoffs. To this end, I formulated formulated the following five scientific hypotheses:

- H1: Participants would report lower delta SSQ scores with the adaptive and symmetric restrictors compared to the control condition without restriction.

- H2: Participants would report lower discomfort scores with the adaptive and symmetric restrictors compared to the control condition.
- H3: Participants would be immersed in the navigation task longer with the adaptive restrictor and symmetric restrictor compared to the control condition.
- H4: Participants would report better visibility with the adaptive restrictor and control condition compared to the symmetric restrictor.
- H5: Participants would report a greater sense of presence with the adaptive restrictor and control condition compared to the symmetric restrictor.

6.6 Results

Shapiro-Wilk tests indicated violations of normality for cybersickness, discomfort, and task performance measures. Therefore, all variables were analyzed using non-parametric tests, and descriptive statistics are reported as median (Mdn) and interquartile range (IQR). Friedman tests were conducted using a significance value of $\alpha = .05$. When significant differences were found, post-hoc analyses were conducted using Conover tests with a Holm-Bonferroni correction for multiple comparisons. Because no significant effects were found between the two virtual environment types across all our measures, these analyses were not included in our results.

Cybersickness. Results for the delta overall SSQ scores are shown in Figure 6.7. A Friedman test revealed a significant difference among the three FOV conditions, $\chi^2(2) = 8.78$, $p = .01$. Post hoc analysis showed that the Adaptive Restrictor ($Mdn = 41.14$, $IQR = 53.29$) resulted in significantly lower delta SSQ scores compared with the None condition ($Mdn = 71.06$, $IQR = 37.40$), $p = .01$. The Symmetric restrictor ($Mdn = 57.97$, $IQR = 41.14$) was not significantly different

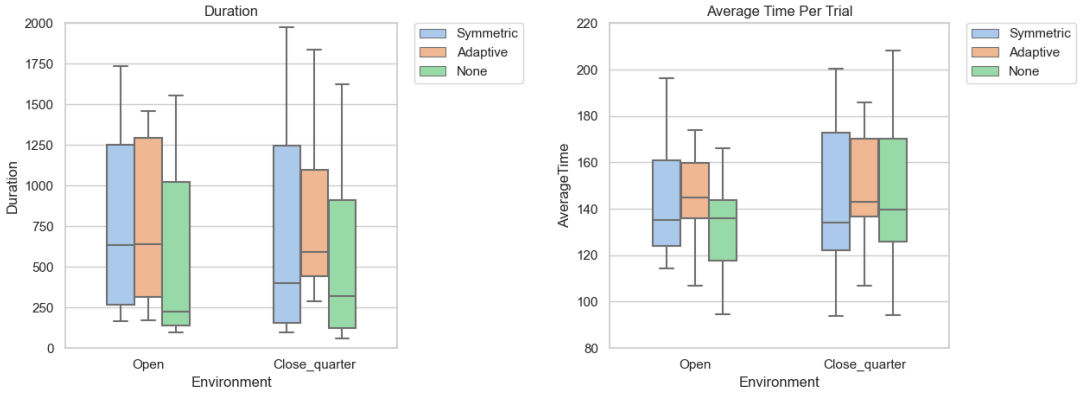

(a) (b)

Figure 6.9: (a) Box plots of immersion duration for each condition. (b) Box plots of average immersion time in each trial for each condition. Participants using the adaptive restrictor persisted significantly longer in the virtual environment compared to the unrestricted condition.

from the None condition, $p = .31$, or the Adaptive restrictor, $p = .12$. These results partially support hypothesis H1.

Discomfort Scores. Results for the average and relative discomfort scores are shown in Figure 6.8. Analysis of ADS ratings using a Friedman test did not reveal any significant differences among the three FOV conditions, $\chi^2(2) = 1.02, p = .60$. However, for RDS ratings, the analysis was significant, $\chi^2(2) = 20.16$, $p < .001$. Post hoc comparisons indicated that the Adaptive restrictor ($Mdn = 7.48$, $IQR = 3.13$) was significantly more comfortable than the None condition ($Mdn = 9.04$, $IQR = 2.71$), $p < .001$. The Symmetric condition ($Mdn = 8.53$, $IQR = 4.62$) was also more comfortable than the None condition, $p = .01$. However, RDS ratings for the Adaptive and the Symmetric restrictors were not significantly different, $p = .14$. The results for relative discomfort scores support hypothesis H2.

Task Performance. Results for overall task duration and average time per trial are shown in Figure 6.9. A Friedman test for task duration revealed significant

differences among the three FOV conditions, $\chi^2(2) = 9.53$, $p < .01$. Post hoc comparisons indicated participants remained immersed in the navigation task significantly longer using the Adaptive restrictor ($Mdn = 618.36$, $IQR = 747.58$) compared to the None condition ($Mdn = 299.60$, $IQR = 865.18$), $p = .01$. The Symmetric restrictor ($Mdn = 490.79$, $IQR = 1015.26$) was not significantly different from either the Adaptive restrictor, $p = .43$, or the None condition, $p = .06$.

A Friedman test for average times spent to complete each trial was not significant, $\chi^2(2) = 2.39$, $p = .30$. However, for the number of completed trials, this analysis revealed significant differences among the three FOV conditions, $\chi^2(2) = 17.56$, $p < .001$. Post hoc comparisons indicated that compared to the None condition, participants completed significantly more trials when using either the Adaptive restrictor, $p < .001$, or the Symmetric restrictor, $p = .03$. The Adaptive and Symmetric restrictor conditions were not significantly different, $p = 0.09$. Taken together, these results partially support hypothesis H3.

Subjective Experience. Results from the feedback questionnaire are shown in Figure 6.10. A Friedman test revealed significant differences in visibility ratings among the three FOV conditions, $\chi^2(2) = 22.97$, $p < .001$. Post-hoc analysis indicated that visibility ratings were higher in the None condition ($Mdn = 6.00$, $IQR = 1.00$) compared to both the Adaptive restrictor ($Mdn = 4.00$, $IQR = 2.00$), $p =< .001$, and Symmetric restrictor ($Mdn = 3.00$, $IQR = 2.75$), $p =< .001$. However, the difference between the Adaptive and Symmetric restrictors was not significant, $p = .58$. These results partially support hypothesis H4.

A Friedman test of the presence ratings also revealed significant differences among the three FOV conditions, $\chi^2(2) = 17.40$, $p < .001$. Post-hoc analysis indicated that the Symmetric restrictor ($Mdn = 4.00$, $IQR = 1.75$) received significantly lower presence ratings compared to both the Adaptive restrictor ($Mdn = 5.50$, $IQR = 1.00$), $p < .01$, and the None condition ($Mdn = 6.00$, $IQR = 1.00$), $p < .001$. Presence ratings for the Adaptive restrictor and None condition were not significantly different, $p = .28$. These results fully support

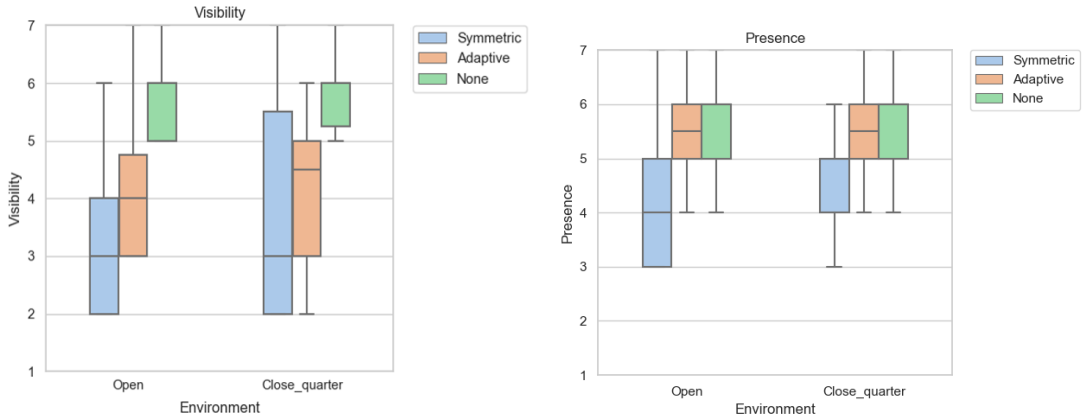

(a) (b)

Figure 6.10: (a) Box plots of the visibility. The direction of the scale was adjusted so that higher values are associated with positive outcomes. Users reported significantly better visibility when using unrestricted condition compared to the Adaptive restrictor and the Symmetric restrictor. (b) Box plots of the sense of presence. Users reported a significantly higher sense of presence when using the Adaptive restrictor and unrestricted condition compared to the Symmetric restrictor.

hypothesis H5.

6.7 Discussion

6.7.1 Effects on Cybersickness and Discomfort

The results for both the delta SSQ scores and relative discomfort ratings indicated that the adaptive restrictor was effective in mitigating negative symptoms compared to the control condition without FOV restriction. Because both restrictor conditions restrict the optical flow visible to the participant during virtual movement, we did not have any a priori hypotheses that one would outperform the other on comfort measures. Although it is interesting to note that SSQ scores

for the symmetric restrictor were generally observed to lie in between the adaptive and control conditions, these results were statistically inconclusive, and no scientific conclusions can be drawn from these data. These results are consistent with the original FOV restriction experiment reported by Fernandes and Feiner, in which the symmetric restrictor provided benefits for relative discomfort ratings, but not SSQ scores [5].

Since average discomfort scores were computed from only the trials that were completed, a participant who quit early may have scores that are not directly comparable to a participant who finished all trials. Therefore, the ADS is only meaningful if most of the participants completed a consistent number of trials. Given the wide distribution of the number of trials completed by participants in my experiment, the relative discomfort scores provide a more reliable basis for comparison. These results are consistent with prior studies (e.g., [5, 13, 14]) and provide further evidence that it may not be useful to analyze ADS in future experiments using this protocol unless all participants complete the same number of trials.

6.7.2 Effects on Task Performance

Participants using the adaptive restrictor remained immersed for significantly longer in the virtual environment than the unrestricted condition. Because participants were explicitly instructed to stop if they felt motion sickness and the task ended immediately upon entering a discomfort score of 10, the longer immersion time was further evidence that the adaptive restrictor was effective in mitigating negative effects. In addition, no significant effects were found for the three restriction conditions in the average time participants took to complete each trial, so I did not find any empirical evidence supporting an alternative explanation based on differences in movement speed through the maze.

6.7.3 Effects on Subjective Experience

Participants rated their visibility significantly higher in the unrestricted control condition compared to both the adaptive and symmetric restrictors. This is an expected result, because the use of FOV restriction necessarily entails finding an acceptable tradeoff between visibility and discomfort. Although the subjective ratings of visibility between the two restrictors were not significant, the adaptive restrictor produced significantly higher presence ratings. This is an encouraging result that may be explained by examining the quantitative logs of the displayed FOV during each frame. When the adaptive restricor was applied, participants were shown a median value of 90.88° horizontal FOV and 90.87° vertical FOV in the close-quarter environment. In the open environment, the median value was 94.40° for the horizontal FOV and 78.54° for the vertical FOV. Because the symmetric restrictor provided approximately 60° FOV in both environments, the adaptive restrictor occluded less of the visual field while providing similar benefits in mitigating cybersickness and general discomfort.

6.7.4 Limitations

The adaptive restriction technique has several limitations that may be addressed in future work. Consistent with prior implementations of FOV restriction, the occluding mask was shaped as an ellipse. However, the boundaries between the regions with the high and low optical flow may form an irregular shape within the user's visual field, and an ellipse may not an ideal geometric approximation. On the other hand, a mask that more precisely fits within the low optical flow regions can have complex, non-convex contours, which may result in undesirable visual artifacts. In general, the effects of non-elliptical FOV restrictors have not been investigated and remain an open question for future work.

In this study, the center of the adaptive restrictor was changed based on the optical flow computed from the visual scene. Our implementation is compatible with a wide variety of consumer VR systems, and we imposed general constraints

on the restrictor size and position to prevent it from shifting too far from the center or blocking too much of the visual field. However, when targeting a headset with real-time eye tracking, we believe that adaptive restriction could be further improved by considering the user's gaze direction in combination with optical flow.

6.8 Conclusion

In this chapter, I proposed and evaluated adaptive FOV restriction, a novel variant of a widely used technique for mitigating cybersickness in virtual reality applications. I conducted a mixed design user study with three conditions and two environments to compare the proposed technique with a traditional symmetric restrictor and a control condition without FOV restriction. The results indicated that adaptive restrictor was effective in mitigating cybersickness and reducing subjective discomfort, while simultaneously supporting a better sense of presence than the symmetric restrictor. In general, I found no empirical evidence that suggests potential drawbacks of applying the adaptive restrictor over the traditional symmetric implementation. Therefore, I conclude that adaptive FOV restriction based on real-time measurement of optical flow is a promising approach, especially for virtual reality applications that involve transitioning between indoor and outdoor scenes with varying visual characteristics.

Algorithm 1 A pipeline to create adaptive field-of-view restriction

1: Compute the optical flow in the x and y directions using a simplified version of the Horn–Schunck algorithm optimized for use in a real-time shader and output the optical flow texture [115, 116].
2: Divide the optical flow texture into 32 × 32 grids (1024 grids in total) and use the maximum optical flow value within each grid to represent the optical flow value of this grid. The output is a 32 × 32 ARGB texture.
3: **for** Each pixel in the texture **do**
4: **if** pixel's optical flow < threshold **then**
5: The alpha channel of the pixel is 0
6: **else**
7: The alpha channel of the pixel is 1
8: Use the connected-component labelling to connect pixels with alpha channel equal to 0.
9: Find the largest connected region.
10: Approximate the largest connected region as an ellipse region and calculate the center c and approximate radius r of the region.
11: $c_x = Clamp(c_x, c_{screen_x} - c_{offset_l}, c_{screen_x} + c_{offset_r})$
12: $c_y = Clamp(c_y, c_{screen_y} - c_{offset_d}, c_{screen_y} + c_{offset_u})$
13: **if** $c_{screen_x} > c_x$ **then**
14: $x_{offset} = (c_{screen_x} - c_x)/c_{offset_l}$
15: **else**
16: $x_{offset} = (c_{screen_x} - c_x)/c_{offset_r}$
17: **if** $c_{screen_y} > c_y$ **then**
18: $y_{offset} = (c_{screen_y} - c_y)/c_{offset_d}$
19: **else**
20: $y_{offset} = (c_{screen_y} - c_y)/c_{offset_u}$
21: Calculate the minimum restrictor radius r_{min} based on the restrictor center c using the following equation $r_{min} = w \cdot \sqrt{c^2_{offset_x} + c^2_{offset_y}} \cdot r_{min}$
22: Calculate the restrictor radius $r = max(r, r_{min})$
23: Apply r as the inner radius of the restrictor, then add 0.1 to form the outer radius.

Chapter 7

Conclusion and Future Work

7.1 Conclusion

In this dissertation, I present a variety of dynamic field-of-view restriction variants for reducing cybersickness in virtual reality when virtual motion is present. Although dynamic field-of-view restriction is a useful technique for reducing cybersickness, it could also be problematic. The traditional symmetrical design trades off the user's visibility and presence in exchange for relief from discomfort. The feature that the restrictor is driven by virtual velocity may also introduce additional discomfort due to texture changes. The restrictor design I suggest shows promise for enhancing subjective experience while retaining a strong capacity to lessen discomfort.

A **passthrough FOV restrictor**, described in Chapter 3, combines dynamic FOV modification with a wireframe mesh that was generated from a 3D scan of the physical environment. With this technique, users can experience the benefits of reducing motion sickness while also maintaining awareness of their location in the physical world.

A **ground-visible restrictor**, described in Chapter 4, uses an asymmetric mask that obscures the upper and side regions of the periphery but leaves the lower region unoccluded. This technique can improve user comfort during virtual

locomotion, and also provides benefits for postural stability and subjective sense of presence. To the best of my knowledge, this is the first study about the effects of restricting different peripheral regions of the FOV on cybersickness.

A **side restrictor**, described in Chapter 5, that an asymmetric mask that obscures only one side region of the periphery during virtual rotation. This technique maintains similar outstanding benefits for improving user comfort compared to the symmetric restriction while providing better performance for cybersickness reduction, visibility, and immersion time during virtual times.

An **adaptive restrictor**, described in Chapter 6, which preserves perceptual cues for lower optical flow in the user's vision. This technique has a similar favorable ability to reduce discomfort in both close-quarter and open virtual environments while obscuring less of the field of view, having better visibility and sense of presence compared to the symmetric restrictor.

7.2 Design Considerations

Based on my study into FOV restriction techniques in immersive virtual environments, I recommend the following considerations when designing virtual reality applications for head-mounted displays. Because the selection of an appropriate FOV restriction technique is determined by the virtual environments and virtual movements, it is up to the developers of a virtual reality application to determine which scenarios are most relevant. As a result, these suggestions may assist developers to weigh the potential benefits of a FOV restriction technique against any tradeoffs or limitations. In the meantime, designers should also consider giving users the ability to switch the FOV restriction on or off as needed.

7.2.1 Dense Virtual Environment

Dense virtual environments often contain complex visual cues. In such environments, users who perform virtual movements will be susceptible to generating

the mismatch between virtual motion and physical motion. The usage of a FOV restrictor in such cases is expected to improve the user's comfort. Therefore, different types of FOV restrictors can be used depending on the movement types.

Frequent Virtual Forward Movements

The study of chapter 4 showed that the ground-visible restrictor allowed participants to have better user comfort compared to the unrestricted condition and the symmetric restrictor. Furthermore, in the results of chapter 4, users with the ground-visible restrictor have less discomfort than users with a symmetric restrictor. Thus, for applications where users need to navigate through a virtual close-quarter environment with frequent forward movements, the ground-visible restrictor may provide the best performance. These results are widely applicable since forward virtual movement is a general navigation technique for virtual environments across many application domains. However, the virtual environment has a visible and flat ground when walking in my study, and this can help the user to better maintain body balance. So this consideration may not apply to virtual environments with the curved ground or where the ground is covered by obstacles.

Frequent Virtual Turning

In the study of chapter 5, the results showed that the side-restrictor maintains similar outstanding benefits for improving user comfort compared to the symmetric restriction while providing better performance for cybersickness reduction, visibility, and immersion time during virtual times. In addition, the side restrictor was only applied during virtual turning and the symmetric restrictor was applied during forwarding and backward movements in the study. Therefore, for tasks that involve frequent virtual turning, I recommend that the side restrictor provides a better user experience during virtual turning, while the symmetric restrictor can provide similar benefits in other virtual movements.

Mixed Virtual and Physical Movements

The passthrough FOV restriction showed a promising result of keeping users safe from obstacles in the physical environment while reducing users' cybersickness in chapter 3. In the test, I observed that users tend to physically walk unconsciously, even when they didn't need to do so. Given the results and observations, I conclude that displaying a 3D reconstruction of the physical environment at the periphery of the user's FOV during the virtual experience may be beneficial in keeping the user safe while experiencing the virtual application. I recommend that this technique will be suitable for applications where users may need to mix virtual and physical walking, and where users experience virtual reality applications in a physical room of limited size.

7.2.2 Sparse Virtual Environment

Unlike dense environments, sparse environments usually have larger areas and broader views, as well as more sparse visual objects. In such an environment, if the restrictor is more frequently shown up, the pattern in the restrictor may cause more intensive discomfort, as in the results of the symmetric restrictor usage in chapter 4. In chapter 6, users showed reduced cybersickness and better comfort when using the adaptive restrictor and immersed longer in the virtual environment than the unrestricted condition in a large and open environment. In addition, the adaptive restrictor also provided a better sense of presence compared to the symmetric restrictor in the open environment. Therefore, if the application is aimed at PC-based VR devices, I recommend that the adaptive restrictor should be beneficial for users to have better user comfort in sparse virtual environments. However, since it consumes a large amount of resources and is currently a challenge to achieve good frame rates on mobile devices, I recommend considering a new restrictor for applications on mobile VR devices based on the behavior of adaptive restrictor in sparse environments, which blocks the left and right parts in the lower region of the periphery, although further investigation would be needed to validate

this hypothesis.

7.2.3 Frequent Dense-Sparse Transitions

The study in chapter 6 measured the performance of the adaptive restrictor in both close-quarter and open virtual environments, and the results indicated that users with the adaptive restrictor were able to change size and position along with the environment and can successfully reduce cybersickness and improve comfort in both virtual environments, Meanwhile, the adaptive restrictor provides larger FOV than the symmetric restrictor, especially in the open environment. Therefore, if the application is aimed at PC-based VR devices, I suggest that for virtual environments where users need to frequently switch between indoors and outdoors, the adaptive restrictor may accommodate changes in the virtual environment easily and provide a better user experience. For mobile VR devices, I suggest switch the restrictor between multiple asymmetric restrictor based on the scene and movements.

7.3 Future Work

In the future, there is ample potential for the design of FOV restrictions to be further investigated. I will discuss three major categories for future research in FOV restriction.

7.3.1 Passthrough FOV Restriction

As discussed in Chapter 3, it is possible to implement the proposed technology in a headset with real-time 3D scanning capabilities, when inside-out tracking and environment mapping technologies will be increasingly integrated with consumers' virtual and augmented reality devices. By leveraging real-time 3D scanning, the benefits of collision avoidance will be introduced for dynamic obstacles and walls. Furthermore, other parameters of the restriction could also be investigated based

on physical movement in the real world, such as the visual appearance of the wireframe mesh (e.g., color, line thickness, etc.).

Although I conducted a test to confirm the feasibility of this technique, there is no study conducted to evaluate the performance of this technique yet. A scientific study is desired to compare the performance of this technique to the symmetric restrictor and the unrestricted condition to demonstrate its ability to reduce cybersickness and prove that this technology allows users to get relief from cybersickness while remaining in the physical environment.

Real-time scanning and 3D reconstruction may be expensive techniques for wireless head-mounted displays. Therefore, other techniques of object detection can also be applied, such as LIDAR, infrared sensors, etc. Users can be alerted when they are near an obstacle by changing the color or shade of the restrictor.

In addition, other rest frame representations will be explored to take full advantage of the FOV restriction mask.

7.3.2 Comprehensive Scientific Evaluation of Asymmetric Restriction

The ground-visible restrictor specifically evaluated the effects during forwarding and backward locomotion, and the side restrictior specifically explored the effects during virtual turning. These techniques have not been thoroughly investigated during different types of movement, such as up-to-down shifting. It is reasonable to assume that other forms of asymmetric restrictions that mask the upper and lower periphery in different ways may provide benefits in a forward and backward motion.

In addition, the combination of different asymmetric restrictors for translation and turns, such as side restriction, foveated restriction [96], and ground-visible restriction [13], has yet to be investigated. Future studies can also investigate FOV restriction techniques in a wider range of virtual environments and tasks to further understand the applicability of these techniques in different types of VR

applications.

In the user study of Chapter 4, the relationship between the cybersickness mitigation and postural sway was investigated. In the future, I also plan to further investigate the relationship between cybersickness mitigation interventions and postural stability, including postural precursors before and during virtual reality exposure.

7.3.3 Adaptive Restriction Techniques

The work presented in Chapter 6 proposed a restrictor whose size and position can be adjusted according to the amount of optical flow generated by users' movements. It therefore can be adaptive to different virtual environments and virtual velocities. The level of cybersickness is related to many factors, which in turn can be used to determine the shape and size of the restrictor. Future studies can also investigate new variants and parameters for FOV restriction techniques capable of adapting themselves to virtual environments or users. For example, there are a variety of continuous objective measures that can be used as input to adjust the FOV restriction size based on their feedback, such as postural sway, EEG, and heart rate. The position of the FOV to be masked can be determined based on the number of polygons in the mesh of the object displayed in the current view.

In this research, the size and position of the restrictor were scaled by a non-linear function. It will be interesting to simulate the relationship between the optical flow amount and cybersickness level using the machine learning algorithms. Other factors related to cybersickness will also be taken into account in plans to develop technologies that can be more broadly adapted to individual differences.

References

[1] Joseph J LaViola Jr. A discussion of cybersickness in virtual environments. *ACM Sigchi Bulletin*, 32(1):47–56, 2000.

[2] Séamas Weech, Sophie Kenny, and Michael Barnett-Cowan. Presence and cybersickness in virtual reality are negatively related: a review. *Frontiers in psychology*, 10:158, 2019.

[3] Frank Koslucher, Eric Haaland, and Thomas A Stoffregen. Sex differences in visual performance and postural sway precede sex differences in visually induced motion sickness. *Experimental brain research*, 234(1):313–322, 2016.

[4] Mark Bolas, J Adam Jones, Ian McDowall, and Evan Suma. Dynamic field of view throttling as a means of improving user experience in head mounted virtual environments, 2017. US Patent 9,645,395.

[5] Ajoy S Fernandes and Steven K Feiner. Combating vr sickness through subtle dynamic field-of-view modification. In *2016 IEEE Symposium on 3D User Interfaces (3DUI)*, pages 201–210. IEEE, 2016.

[6] Stephen Palmisano, Robert S Allison, Mark M Schira, and Robert J Barry. Future challenges for vection research: definitions, functional significance, measures, and neural bases. *Frontiers in psychology*, 6:193, 2015.

[7] Joel Teixeira and Stephen Palmisano. Effects of dynamic field-of-view restriction on cybersickness and presence in hmd-based virtual reality. *Virtual Reality*, 25(2):433–445, 2021.

[8] Kieran Carnegie and Taehyun Rhee. Reducing visual discomfort with hmds using dynamic depth of field. *IEEE computer graphics and applications*, 35(5):34–41, 2015.

[9] Majed Al Zayer, Isayas B Adhanom, Paul MacNeilage, and Eelke Folmer. The effect of field-of-view restriction on sex bias in vr sickness and spatial navigation performance. In *Proceedings of the 2019 CHI Conference on Human Factors in Computing Systems*, pages 1–12, 2019.

[10] Paulo Bala, Dina Dionísio, Valentina Nisi, and Nuno Nunes. Visually induced motion sickness in 360° videos: Comparing and combining visual optimization techniques. In *2018 IEEE International Symposium on Mixed and Augmented Reality Adjunct (ISMAR-Adjunct)*, pages 244–249. IEEE, 2018.

[11] Colin Groth, Jan-Philipp Tauscher, Nikkel Heesen, Steve Grogorick, Susana Castillo, and Marcus Magnor. Mitigation of cybersickness in immersive 360 videos. In *2021 IEEE Conference on Virtual Reality and 3D User Interfaces Abstracts and Workshops (VRW)*, pages 169–177. IEEE, 2021.

[12] Fei Wu and Evan Suma Rosenberg. Combining dynamic field of view modification with physical obstacle avoidance. In *2019 IEEE Conference on Virtual Reality and 3D User Interfaces (VR)*, pages 1882–1883. IEEE, 2019.

[13] Fei Wu, George S Bailey, Thomas Stoffregen, and Evan Suma Rosenberg. Don't block the ground: Reducing discomfort in virtual reality with an asymmetric field-of-view restrictor. In *Symposium on Spatial User Interaction*, pages 1–10, 2021.

[14] Fei Wu and Evan Suma Rosenberg. Asymmetric lateral field-of-view restriction to mitigate cybersickness during virtual turns. In *2022 IEEE Conference on Virtual Reality and 3D User Interfaces (VR)*, pages 103–111. IEEE, 2022.

[15] Tom Forsyth. VR Sickness, The Rift, and How Game Developers Can Help — Oculus, 2013.

[16] Lisa Rebenitsch and Charles Owen. Review on cybersickness in applications and visual displays. *Virtual Reality*, 20(2):101–125, 2016.

[17] Lawrence J Hettinger and Gary E Riccio. Visually induced motion sickness in virtual environments. *Presence: Teleoperators & Virtual Environments*, 1(3):306–310, 1992.

[18] Behrang Keshavarz, Bernhard E Riecke, Lawrence J Hettinger, and Jennifer L Campos. Vection and visually induced motion sickness: how are they related? *Frontiers in psychology*, 6:472, 2015.

[19] Gary E Riccio and Thomas A Stoffregen. An ecological theory of motion sickness and postural instability. *Ecological psychology*, 3(3):195–240, 1991.

[20] Frank C.Koslucher, Eric J.Haaland, and Thomas A. Stoffregen. Body load and the postural precursors of motion sickness. *Gait & Posture*, 39(1):606–610, jan 2014.

[21] Thomas A. Stoffregen, Elise Faugloire, Ken Yoshida, Moira B. Flanagan, and Omar Merhi. Motion Sickness and Postural Sway in Console Video Games. *Human Factors: The Journal of the Human Factors and Ergonomics Society*, 50(2):322–331, apr 2008.

[22] Justin Munafo, Meg Diedrick, and Thomas A Stoffregen. The virtual reality head-mounted display oculus rift induces motion sickness and is sexist in its effects. *Experimental brain research*, 235(3):889–901, 2017.

[23] Gregory Kramida. Resolving the vergence-accommodation conflict in head-mounted displays. *IEEE transactions on visualization and computer graphics*, 22(7):1912–1931, 2015.

[24] Sheldon M Ebenholtz. Motion sickness and oculomotor systems in virtual environments. *Presence: Teleoperators & Virtual Environments*, 1(3):302–305, 1992.

[25] Stephen Palmisano, Robert S Allison, and Juno Kim. Cybersickness in head-mounted displays is caused by differences in the user's virtual and physical head pose. *Frontiers in Virtual Reality*, 1:24, 2020.

[26] Suzanne AE Nooij, Paolo Pretto, Daniel Oberfeld, Heiko Hecht, and Heinrich H Bülthoff. Vection is the main contributor to motion sickness induced by visual yaw rotation: Implications for conflict and eye movement theories. *PloS one*, 12(4):e0175305, 2017.

[27] Dante Risi and Stephen Palmisano. Effects of postural stability, active control, exposure duration and repeated exposures on hmd induced cybersickness. *Displays*, 60:9–17, 2019.

[28] Jiun-Yu Lee, Ping-Hsuan Han, Ling Tsai, Rih-Ding Peng, Yang-Sheng Chen, Kuan-Wen Chen, and Yi-Ping Hung. Estimating the simulator sickness in immersive virtual reality with optical flow analysis. In *SIGGRAPH Asia 2017 Posters*, pages 1–2. 2017.

[29] Maria Gallagher, Reno Choi, and Elisa Raffaella Ferrè. Multisensory interactions in virtual reality: optic flow reduces vestibular sensitivity, but only for congruent planes of motion. *Multisensory research*, 33(6):625–644, 2020.

[30] Richard HY So, WT Lo, and Andy TK Ho. Effects of navigation speed on motion sickness caused by an immersive virtual environment. *Human factors*, 43(3):452–461, 2001.

[31] Wanjun Chen, JZ Chen, and Richard Hau Yue So. Visually induced motion sickness: Effects of translational visual motion along different axes. *Contemporary ergonomics and human factors*, 2011:281–287, 2011.

[32] Alireza Mazloumi Gavgani, Deborah M Hodgson, and Eugene Nalivaiko. Effects of visual flow direction on signs and symptoms of cybersickness. *PloS one*, 12(8):e0182790, 2017.

[33] Michael E McCauley and Thomas J Sharkey. Cybersickness: Perception of self-motion in virtual environments. *Presence: Teleoperators & Virtual Environments*, 1(3):311–318, 1992.

[34] Robert S Kennedy, Norman E Lane, Kevin S Berbaum, and Michael G Lilienthal. Simulator sickness questionnaire: An enhanced method for quantifying simulator sickness. *The international journal of aviation psychology*, 3(3):203–220, 1993.

[35] Behrang Keshavarz and Heiko Hecht. Validating an efficient method to quantify motion sickness. *Human factors*, 53(4):415–426, 2011.

[36] Jelte E Bos, Sjoerd C de Vries, Martijn L van Emmerik, and Eric L Groen. The effect of internal and external fields of view on visually induced motion sickness. *Applied ergonomics*, 41(4):516–521, 2010.

[37] Xiao Dong, Ken Yoshida, and Thomas A Stoffregen. Control of a virtual vehicle influences postural activity and motion sickness. *Journal of Experimental Psychology: Applied*, 17(2):128, 2011.

[38] Sébastien J Villard, Moira B Flanagan, Gina M Albanese, and Thomas A Stoffregen. Postural instability and motion sickness in a virtual moving room. *Human factors*, 50(2):332–345, 2008.

[39] Dante Risi and Stephen Palmisano. Can we predict susceptibility to cybersickness? In *25th ACM Symposium on Virtual Reality Software and Technology*, pages 1–2, 2019.

[40] Mark S Dennison, A Zachary Wisti, and Michael D'Zmura. Use of physiological signals to predict cybersickness. *Displays*, 44:42–52, 2016.

[41] Pulkit Budhiraja, Mark Roman Miller, Abhishek K Modi, and David Forsyth. Rotation Blurring: Use of Artificial Blurring to Reduce Cybersickness in Virtual Reality First Person Shooters. *arXiv, 1710.02599*, 2017, 1710.02599.

[42] Yun-Xuan Lin, Rohith Venkatakrishnan, Roshan Venkatakrishnan, Elham Ebrahimi, Wen-Chieh Lin, and Sabarish V Babu. How the presence and size of static peripheral blur affects cybersickness in virtual reality. *ACM Transactions on Applied Perception (TAP)*, 17(4):1–18, 2020.

[43] Guangyu Nie, Yue Liu, and Yongtian Wang. Prevention of Visually Induced Motion Sickness Based on Dynamic Real-Time Content-Aware Non-salient Area Blurring. *Adjunct Proceedings of the 2017 IEEE International Symposium on Mixed and Augmented Reality, ISMAR-Adjunct 2017*, pages 75–78, 2017.

[44] Jiun-Yu Lee, Ping-Hsuan Han, Ling Tsai, Rih-Ding Peng, Yang-Sheng Chen, Kuan-Wen Chen, and Yi-Ping Hung. Estimating the simulator sickness in immersive virtual reality with optical flow analysis. *SIGGRAPH Asia 2017 Posters on - SA '17*, pages 1–2, 2017.

[45] Helmut Buhler, Sebastian Misztal, and Jonas Schild. Reducing vr sickness through peripheral visual effects. In *2018 IEEE Conference on Virtual Reality and 3D User Interfaces (VR)*, pages 517–9. IEEE, 2018.

[46] Yasin Farmani and Robert J Teather. Evaluating discrete viewpoint control to reduce cybersickness in virtual reality. *Virtual Reality*, 24(4):645–664, 2020.

[47] Su Han Park, Bin Han, and Gerard Jounghyun Kim. Mixing in reverse optical flow to mitigate vection and simulation sickness in virtual reality. In *CHI Conference on Human Factors in Computing Systems*, pages 1–11, 2022.

[48] Paulo Bala, Ian Oakley, Valentina Nisi, and Nuno Nunes. Staying on track: a comparative study on the use of optical flow in 360 video to mitigate vims. In *ACM International Conference on Interactive Media Experiences*, pages 82–93, 2020.

[49] Hiroshi Watanabe and Hiroyasu Ujike. The activity of iso/study group on "image safety" and three biological effect. In *2008 Second International Symposium on Universal Communication*, pages 210–214. IEEE, 2008.

[50] Cyriel Diels, Kazuhiko Ukai, and Peter A Howarth. Visually induced motion sickness with radial displays: effects of gaze angle and fixation. *Aviation, space, and environmental medicine*, 78(7):659–665, 2007.

[51] Jan-Philipp Stauffert, Florian Niebling, and Marc Erich Latoschik. Effects of latency jitter on simulator sickness in a search task. *IEEE Virtual Reality*, pages 121–127, 2018.

[52] Amelia Kinsella, Ryan Mattfeld, Eric Muth, and Adam Hoover. Frequency, not amplitude, of latency affects subjective sickness in a head-mounted display. *Aerospace Medicine and Human Performance*, 87(7):604–609, 2016.

[53] Matthew E. St. Pierre, Salil Banerjee, Adam W. Hoover, and Eric R. Muth. The effects of 0.2hz varying latency with 20–100ms varying amplitude on simulator sickness in a helmet mounted display. *Displays*, 36:1–8, 2015.

[54] Behrang Keshavarz and Heiko Hecht. Stereoscopic viewing enhances visually induced motion sickness but sound does not. *Presence: Teleoperators and Virtual Environments*, 21(2):213–228, 2012.

[55] Evren Bozgeyikli, Andrew Raij, Srinivas Katkoori, and Rajiv Dubey. Point & teleport locomotion technique for virtual reality. In *Proceedings of the 2016 Annual Symposium on Computer-Human Interaction in Play*, pages 205–216. ACM, 2016.

[56] Roy A. Ruddle, Andrew Howes, Stephen J. Payne, and Dylan M. Jones. Effects of hyperlinks on navigation in virtual environments. *International Journal of Human Computer Studies*, 53(4):551–581, 2000.

[57] Doug A Bowman, David Koller, and Larry F Hodges. Travel in immersive virtual environments: An evaluation of viewpoint motion control techniques. In *Virtual Reality Annual International Symposium*, pages 45–52. IEEE, 1997.

[58] Robert Farmani, Yasin and Teather. Viewpoint Snapping to Reduce Cybersickness in Virtual Reality. *Graphics interface*, pages 159–166, 2018.

[59] Tim WeiBker, Kunert Bernd, F Ohlich, and Alexander Kulik. Spatial Updating and Simulator Sickness during Steering and Jumping in Immersive Virtual Environments. *Ieee Vr*, pages 256–307, 2018.

[60] Sysdia Solutions Ltd. Vrtk_dashteleport. https://vrtoolkit.readme.io/docs/vrtk_dashteleport, 2019. Accessed on 2019-09-27.

[61] M P Jacob Habgood, David Moore, David Wilson, and Sergio Alapont. Rapid, continuous movement between nodes as an accessible virtual reality locomotion technique. *2018 IEEE Virtual Reality (VR)*, pages 1–9, 2018.

[62] Gerard Llorach, Alun Evans, and Josep Blat. Simulator sickness and presence using hmds: comparing use of a game controller and a position estimation system. In *Proceedings of the 20th ACM Symposium on Virtual Reality Software and Technology*, pages 137–140, 2014.

[63] Weiya Chen, Anthony Plancoulaine, Nicolas Férey, Damien Touraine, Julien Nelson, and Patrick Bourdot. 6dof navigation in virtual worlds: comparison of joystick-based and head-controlled paradigms. In *Proceedings of the 19th ACM Symposium on Virtual Reality Software and Technology*, pages 111–114, 2013.

[64] Beverly K Jaeger and Ronald R Mourant. Comparison of simulator sickness using static and dynamic walking simulators. In *Proceedings of the Human Factors and Ergonomics Society Annual Meeting*, volume 45, pages 1896–1900. SAGE Publications Sage CA: Los Angeles, CA, 2001.

[65] Jérémy Plouzeau, Damien Paillot, Jean-Rémy Chardonnet, and Frédéric Merienne. Effect of proprioceptive vibrations on simulator sickness during navigation task in virtual environment. 2015.

[66] Sungchul Jung, Richard Li, Ryan McKee, Mary C Whitton, and Robert W Lindeman. Floor-vibration vr: Mitigating cybersickness using whole-body tactile stimuli in highly realistic vehicle driving experiences. *IEEE Transactions on Visualization and Computer Graphics*, 27(5):2669–2680, 2021.

[67] Jose L. Dorado and Pablo A. Figueroa. Ramps are better than stairs to reduce cybersickness in applications based on a HMD and a Gamepad. *IEEE Symposium on 3D User Interfaces 2014, 3DUI 2014 - Proceedings*, pages 47–50, 2014.

[68] Behrang Keshavarz, Alison C. Novak, Lawrence J. Hettinger, Thomas A. Stoffregen, and Jennifer L. Campos. Passive restraint reduces visually induced motion sickness in older adults. *Journal of Experimental Psychology: Applied*, 23(1):85–99, 2017.

[69] Rohith Venkatakrishnan, Roshan Venkatakrishnan, Reza Ghaiumy Anaraky, Matias Volonte, Bart Knijnenburg, and Sabarish V Babu. A structural equation modeling approach to understand the relationship between control, cybersickness and presence in virtual reality. In *2020 IEEE Conference on Virtual Reality and 3D User Interfaces (VR)*, pages 682–691. IEEE, 2020.

[70] Xiao Dong and Thomas A Stoffregen. Postural activity and motion sickness among drivers and passengers in a console video game. In *Proceedings of the*

Human Factors and Ergonomics Society Annual Meeting, volume 54, pages 1340–1344. SAGE Publications Sage CA: Los Angeles, CA, 2010.

[71] Roshan Venkatakrishnan, Rohith Venkatakrishnan, Ayush Bhargava, Kathryn Lucaites, Hannah Solini, Matias Volonte, Andrew Robb, Sabarish V Babu, Wen-Chieh Lin, and Yun-Xuan Lin. Comparative evaluation of the effects of motion control on cybersickness in immersive virtual environments. In *2020 IEEE Conference on Virtual Reality and 3D User Interfaces (VR)*, pages 672–681. IEEE, 2020.

[72] John F Golding, Kim Doolan, Amish Acharya, Maryame Tribak, and Michael A Gresty. Cognitive cues and visually induced motion sickness. *Aviation, space, and environmental medicine*, 83(5):477–482, 2012.

[73] Eunhee Chang, Hyun Taek Kim, and Byounghyun Yoo. Predicting cybersickness based on user's gaze behaviors in hmd-based virtual reality. *Journal of Computational Design and Engineering*, 8(2):728–739, 2021.

[74] Rifatul Islam, Samuel Ang, and John Quarles. Cybersense: A closed-loop framework to detect cybersickness severity and adaptively apply reduction techniques. In *2021 IEEE Conference on Virtual Reality and 3D User Interfaces Abstracts and Workshops (VRW)*, pages 148–155. IEEE, 2021.

[75] Hak Gu Kim, Wissam J Baddar, Heoun-taek Lim, Hyunwook Jeong, and Yong Man Ro. Measurement of exceptional motion in vr video contents for vr sickness assessment using deep convolutional autoencoder. In *Proceedings of the 23rd ACM Symposium on Virtual Reality Software and Technology*, pages 1–7, 2017.

[76] Jerrold Douglas Prothero. *The Role of Rest Frames in Vection, Presence and Motion Sickness*. PhD thesis, University of Washington, Seattle, 1998.

[77] R. M. Stern, S. Hu, R. B. Anderson, H. W. Leibowitz, and K. L. Koch. The effects of fixation and restricted visual field on vection-induced motion sickness. *Aviation, Space and Environmental Medicine*, 61(8):712–715, 1990.

[78] Henry Been-lirn Duh, Donald E Parker, and Thomas a Furness. An "independent visual background" reduced balance disturbance envoked by visual scene motion. *Proceedings of the SIGCHI conference on Human factors in computing systems - CHI '01*, pages 85–89, 2001.

[79] James Jeng-Weei Lin, Habib Abi-Rached, Do-Hoe Kim, Donald E Parker, and Thomas A Furness. A "natural" independent visual background reduced simulator sickness. In *Proceedings of the human factors and ergonomics society annual meeting*, volume 46, pages 2124–2128. SAGE Publications Sage CA: Los Angeles, CA, 2002.

[80] Frederick Bonato, Andrea Bubka, and Wesley W. O. Krueger. A Wearable Device Providing a Visual Fixation Point for the Alleviation of Motion Sickness Symptoms. *Military Medicine*, 180(12):1268–1272, 2015.

[81] Carolin Wienrich, Christine Katharina Weidner, Celina Schatto, David Obremski, and Johann Habakuk Israel. A virtual nose as a rest-frame-the impact on simulator sickness and game experience. In *2018 10th international conference on virtual worlds and games for serious applications (VS-Games)*, pages 1–8. IEEE, 2018.

[82] EunHee Chang, InJae Hwang, Hyeonjin Jeon, Yeseul Chun, Hyun Taek Kim, and Changhoon Park. Effects of rest frames on cybersickness and oscillatory brain activity. In *2013 International Winter Workshop on Brain-Computer Interface (BCI)*, pages 62–64. IEEE, 2013.

[83] Zekun Cao, Jason Jerald, and Regis Kopper. Visually-induced motion sickness reduction via static and dynamic rest frames. In *2018 IEEE Conference on Virtual Reality and 3D User Interfaces (VR)*, pages 105–112. IEEE, 2018.

[84] Cuiting Guo, Jennifer Ji, and Richard So. Could OKAN be an objective indicator of the susceptibility to visually induced motion sickness? *Proceedings - IEEE Virtual Reality*, pages 87–90, 2011.

[85] Nicholas A. Webb and Michael J. Griffin. Eye movement, vection, and motion sickness with foveal and peripheral vision. *Aviation Space and Environmental Medicine*, 74(6):622–625, 2003.

[86] Isayas Berhe Adhanom, Majed Al-Zayer, Paul Macneilage, and Eelke Folmer. Field-of-view restriction to reduce vr sickness does not impede spatial learning in women. *ACM Transactions on Applied Perception (TAP)*, 18(2):1–17, 2021.

[87] Guang-Yu Nie, Henry Been-Lirn Duh, Yue Liu, and Yongtian Wang. Analysis on mitigation of visually induced motion sickness by applying dynamical blurring on a user's retina. *IEEE transactions on visualization and computer graphics*, 2019.

[88] Young Youn Kim, Eun Nam Kim, Min Jae Park, Kwang Suk Park, Hee Dong Ko, and Hyun Taek Kim. The application of biosignal feedback for reducing cybersickness from exposure to a virtual environment. *Presence: Teleoperators and Virtual Environments*, 17(1):1–16, 2008.

[89] Nahal Norouzi and Greg Welch. Assessing Vignetting as a Means to Reduce VR Sickness During Amplified Head Rotations. *ACM Symposium on Applied Perception*, 2018.

[90] J.D. D Moss and E.R. R Muth. Characteristics of head mounted displays and their effects on simulator sickness. *Human Factors*, 53(3):308–319, 2011.

[91] Nupur Kala, Kyungmin Lim, Kwanghyun Won, Jaesung Lee, Tammy Lee, Sehoon Kim, and Wonhee Choe. P-218: An Approach to Reduce VR Sickness by Content Based Field of View Processing. *SID Symposium Digest of Technical Papers*, 48(1):1645–1648, 2017.

[92] Yue Wei, Jiayue Zheng, and Richard H. Y. So. Allocating less attention to central vision during vection is correlated with less motion sickness. *Ergonomics*, 61(7):933–946, 2018.

[93] Sander Edward Michiel Jansen, Alexander Toet, and Nicolaas Johannes Delleman. Restricting the vertical and horizontal extent of the field-of-view: effects on manoeuvring performance. *The Ergonomics Open Journal*, 3(1), 2010.

[94] Sehoon Kim, Seungheon Lee, Nupur Kala, Jaesung Lee, and Wonhee Choe. An effective fov restriction approach to mitigate vr sickness on mobile devices. *Journal of the Society for Information Display*, 26(6):376–384, 2018.

[95] William Panlener, David M Krum, and J Adam Jones. Effects of horizontal field of view extension on spatial judgments in virtual reality. In *2019 SoutheastCon*, pages 1–7. IEEE, 2019.

[96] Isayas Berhe Adhanom, Nathan Navarro Griffin, Paul MacNeilage, and Eelke Folmer. The effect of a foveated field-of-view restrictor on vr sickness. In *2020 IEEE Conference on Virtual Reality and 3D User Interfaces (VR)*, pages 645–652. IEEE, 2020.

[97] IGN. Eagle flight review. `https://www.youtube.com/watch?v=W2LrzcZCBOE`. Accessed: 2021-03-17.

[98] Jason D Moss and Eric R Muth. Characteristics of head-mounted displays and their effects on simulator sickness. *Human factors*, 53(3):308–319, 2011.

[99] Nahal Norouzi, Gerd Bruder, and Greg Welch. Assessing vignetting as a means to reduce vr sickness during amplified head rotations. In *Proceedings of the 15th ACM Symposium on Applied Perception*, pages 1–8, 2018.

[100] Erica M Barhorst-Cates, Kristina M Rand, and Sarah H Creem-Regehr. The effects of restricted peripheral field-of-view on spatial learning while navigating. *PloS one*, 11(10):e0163785, 2016.

[101] Bing Wu, Teng Leng Ooi, and Zijiang J He. Perceiving distance accurately by a directional process of integrating ground information. *Nature*, 428(6978):73–77, 2004.

[102] Kathleen Turano, Susan J Herdman, and Gislin Dagnelie. Visual stabilization of posture in retinitis pigmentosa and in artificially restricted visual fields. *Investigative ophthalmology & visual science*, 34(10):3004–3010, 1993.

[103] Robert Patterson, Marc D Winterbottom, and Byron J Pierce. Perceptual issues in the use of head-mounted visual displays. *Human factors*, 48(3):555–573, 2006.

[104] Thomas A Stoffregen, Fu-Chen Chen, Manuel Varlet, Cristina Alcantara, and Benoît G Bardy. Getting your sea legs. *PLoS One*, 8(6):e66949, 2013.

[105] Justin Munafo, Christopher Curry, Michael G Wade, and Thomas A Stoffregen. The distance of visual targets affects the spatial magnitude and multifractal scaling of standing body sway in younger and older adults. *Experimental brain research*, 234(9):2721–2730, 2016.

[106] Luke Thompson. VR Tunnelling Pro. `http://www.sigtrapgames.com/VrTunnellingPro/html/`, 2017. Accessed on 12-01-2020.

[107] A Fleming Seay, David M Krum, Larry Hodges, and William Ribarsky. Simulator sickness and presence in a high fov virtual environment. In *Proceedings IEEE Virtual Reality 2001*, pages 299–300. IEEE, 2001.

[108] James J Cummings and Jeremy N Bailenson. How immersive is enough? a meta-analysis of the effect of immersive technology on user presence. *Media Psychology*, 19(2):272–309, 2016.

[109] Jack MH Beusmans. Optic flow and the metric of the visual ground plane. *Vision research*, 38(8):1153–1170, 1998.

[110] Jonathan S Matthis and Brett R Fajen. Visual control of foot placement when walking over complex terrain. *Journal of experimental psychology: human perception and performance*, 40(1):106, 2014.

[111] Sergey Smurov. Qmaze. `https://assetstore.unity.com/packages/tools/modeling/qmaze-30600/`, 2018. Accessed on 12-01-2020.

[112] Christopher Curry, Nicolette Peterson, Ruixuan Li, and Thomas A Stoffregen. Postural precursors of motion sickness in head-mounted displays: drivers and passengers, women and men. *Ergonomics*, 63(12):1502–1511, 2020.

[113] Halim Hicheur, Stéphane Vieilledent, and Alain Berthoz. Head motion in humans alternating between straight and curved walking path: combination of stabilizing and anticipatory orienting mechanisms. *Neuroscience letters*, 383(1-2):87–92, 2005.

[114] Nicholas A Webb and Michael J Griffin. Eye movement, vection, and motion sickness with foveal and peripheral vision. *Aviation, space, and environmental medicine*, 74(6):622–625, 2003.

[115] Berthold KP Horn and Brian G Schunck. Determining optical flow. *Artificial intelligence*, 17(1-3):185–203, 1981.

[116] mattatz. unity-optical-flow. `https://github.com/mattatz/unity-optical-flow`, Accessed: 2022-01-14.